UNIVERSITÄT
BERN

OESCHGER CENTRE
CLIMATE CHANGE RESEARCH

Coupling EM-DAT Reported Flash Floods with IMERG Precipitation Data

Master's Thesis

Leonardo Quirino Olvera

`Student ID: 20-109-609`

Oeschger Centre for Climate Change Research
Universität Bern

Supervisors:
Prof. Dr. Eric Strobl
Dr. Alessio Ciullo

Advisor:
Dr. Dino Collati

February 7, 2024

Declaration of consent

on the basis of Article 30 of the RSL Phil.-nat. 18

Name/First Name: Leonardo Quirino Olvera

Registration Number: 20-109-609

Study program: Master's in Climate Sciences

Bachelor ☐ Master ☑ Dissertation ☐

Title of the thesis: Coupling EM-DAT Reported Flash Floods with IMERG Precipitation Data

Supervisor: Prof. Dr. Eric Strobl and Dr. Alessio Ciullo

I declare herewith that this thesis is my own work and that I have not used any sources other than those stated. I have indicated the adoption of quotations as well as thoughts taken from other authors as such in the thesis. I am aware that the Senate pursuant to Article 36 paragraph 1 litera r of the University Act of 5 September, 1996 is authorized to revoke the title awarded on the basis of this thesis.

For the purposes of evaluation and verification of compliance with the declaration of originality and the regulations governing plagiarism, I hereby grant the University of Bern the right to process my personal data and to perform the acts of use this requires, in particular, to reproduce the written thesis and to store it permanently in a database, and to use said database, or to make said database available, to enable comparison with future theses submitted by others.

Bern, Switzerland, 05.02.2023

Place/Date

Signature

Acknowledgements

This research was supported by funding from the RECEIPT-EU project and Consejo Nacional de Humanidades, Ciencias y Tecnologías.

I express my gratitude to my supervisors Prof. Dr. Eric Strobl, Dr. Alessio Ciullo, and my advisor Dr. Dino Collati, without them this thesis would not have been possible. I want to express my sincere gratitude to the Oescgher Centre for Climate Change Research staff, the Institute of Geography, and the UniS department. Big thanks to Prof. Dr. Olivia Romppainen-Martius, for her invaluable guidance and support throughout this research. I would also like to thank Dr. Fátima Maciel Carrillo González for her assistance and support throughout this whole process. Finally, I would like to thank all my family, friends, and those who have supported me during this endeavor.

Abstract

Flash floods significantly impact societies and their economies. The latest entry of a major flash flood in the Emergency Database is the Democratic Republic of the Congo, with 201,000 USD in total damages, around 20,000 affected people, and 2,970 deaths (Updated 2023-09-26 by UNICEF (2023)). Riverine floods typically affect most people, but flash floods have a higher mortality per incident (Jonkman, 2005), making them extremely dangerous. This research investigates the global distribution and economic impact of flash floods using the EM-DAT database from 2001 to 2020. We introduce a method for georeferencing the EM-DAT entries locating and characterizing each possible flash flood. This study also identifies the Mediterranean Basin, Central South Asia & Georgia, and Southeast Asia as regions most susceptible to flash floods. We found that the spatial distribution of flash floods aligns with the regions affected by monsoonal rainfall patterns.

Contents

Chapter 1

Introduction

Flash Floods occur all over the world and directly impact our societies. Extreme precipitation events can profoundly impact human settlements. In the 2000 - 2019 period, hydrometeorological phenomena were the most common type of natural disaster. According to the United Nations Office for Disaster Risk Reduction (2020), there were 3,254 significant floods in the 2000 - 2019 period (44% of all disasters), and they affected 1.65 billion people (41% of all those affected). In addition, there are 163 floods on average per year, and they can cause significant damage to homes, businesses, and infrastructure. On the national level, for example, Bernet et al. (2017) from 1999 to 2013, surface water floods caused 45% of all insurance claims for localized flood damage in Switzerland. Additionally, le Polain de Waroux (2011) mentions that low-income nations frequently have endemic populations of many epidemic-prone diseases that pose a particular risk during floods; meanwhile, flood-related psychiatric disorders have been increasingly reported in high-income countries.

Figure 1.1: Flash Flood in the Democratic Republic of the Congo in 2023. Source: UNICEF (2023)

According to United Nations Office for Disaster Risk Reduction (2020), over the last 20 years, China has experienced the highest impact of flooding among all countries, averaging 20 floods annually. The effects of flooding in China have been widespread, affecting an estimated 900 million people. With an average of 17 yearly flood events, India is the second most affected country, with around 345 million people affected by floods. Unfortunately, India has also been home to some of the deadliest floods in recent history. For instance, the June 2013 floods in India claimed 6,054 lives. Meanwhile, the July 2010 floods in Pakistan resulted in 1,985 deaths, and the May 2004 floods in Haiti caused 2,665 fatalities. Human settlements are often located in flood-prone areas, which is why flash floods may displace people or cause fatalities. The latest entry of a major flash flood in 2023 is the Democratic Republic of the Congo, with 201,000 USD in total damages, around 20,000 affected people, and 2,970 deaths (Updated 2023-09-26), as the UNICEF (2023) shows in Figure 1.1.

Extreme precipitation events can have a profound impact on human settlements. The most disadvantaged are especially vulnerable to extreme weather because they live and labor in industries where natural hazards tend to occur (INSURESILIENCE, 2016). These events may lead to flash floods, which can cause significant damage to homes, businesses, and infrastructure. Disaster preparedness may take the form of financial tools to help mitigate the impacts and boost the reconstruction/repairs that may be needed. Correctly assessing the occurrence of these disasters depends on developing instruments to diversify such risks. One way to mitigate the impact of extreme precipitation events on a global scale is through international cooperation and pool risk diversification. River floods typically affect most people, but flash floods have a higher mortality per incident (Jonkman, 2005).

Typically, thunderstorm formation in the tropics results from regional/local convection, either by physical or thermodynamic processes, which create local or mesoscale super-cells. These cells may have a life span of several hours and a horizontal extension of ≈ 20 km (Stull, 1988). Most flash flooding is brought on by thunderstorms that move slowly, thunderstorms that pass over the same area repeatedly, or heavy rain from tropical storms and hurricanes. These storms are the leading cause of weather-related deaths in the United States of America (National Weather Service, 2022). These storms spread over a broad spatial and temporal resolution shown in Figure 1.2. Some can be an isolated storm, and others can be up to a synoptic scale.

Software like CLIMADA enables users to model and examine how earthquakes, floods, and other natural catastrophes affect infrastructure and human populations. It employs complex modeling techniques to produce probabilistic

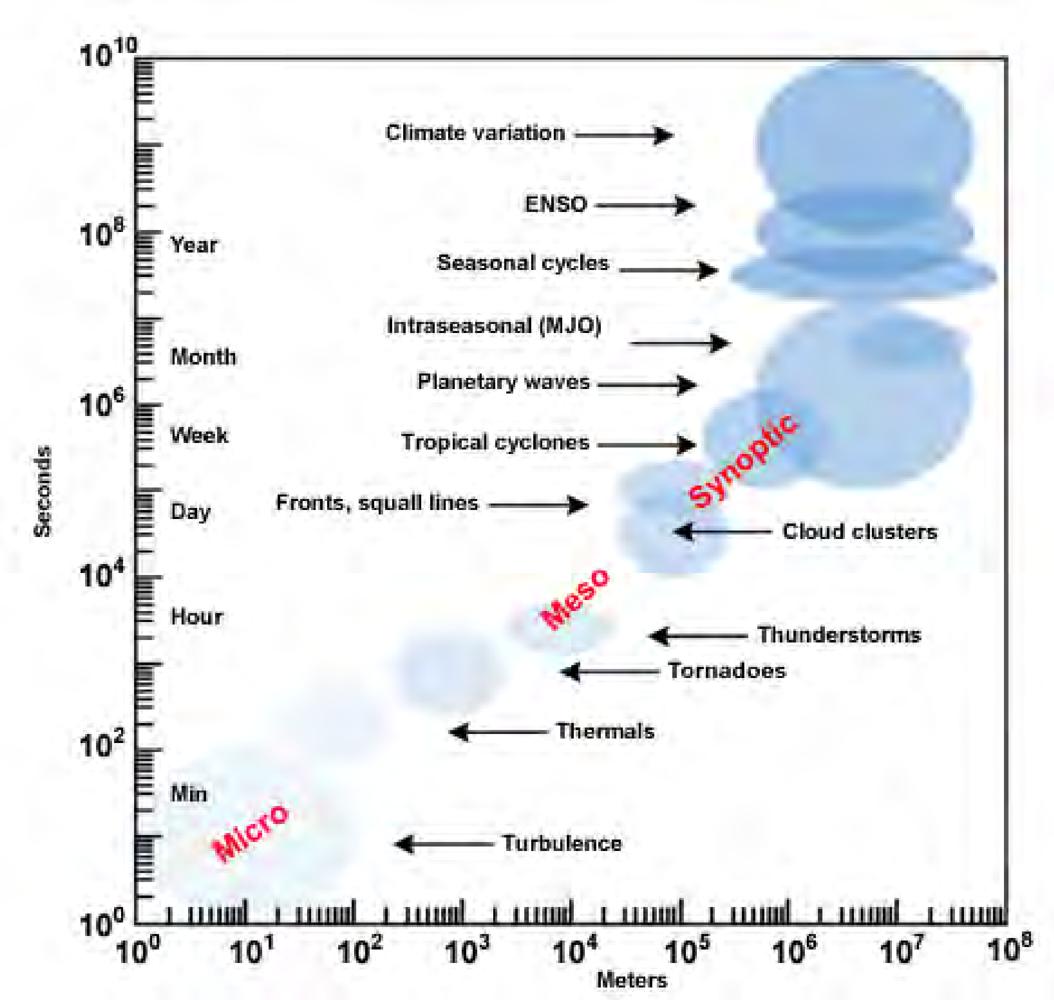

Figure 1.2: Temporal and Spatial Scale of Weather and Climate Phenomena. Source: UCAR/COMET (2011).

risk assessments based on various input data, including weather patterns, geographic features, and demographic data. CLIMADA (2023) is an example of combining precipitation historical data, satellite images, and river flooding simulations to assess potential impacts. Koks and Thissen (2016) simulated three flooding events encompassing the Rotterdam area. In their conclusions, the Rotterdam case demonstrates unequivocally that areas beyond the impacted region are indirectly affected by the natural disaster. Both demonstrate that given the unavoidable nature of flash floods in various regions, it becomes imperative to establish early warning systems, resilient infrastructure, and post-disaster financial mechanisms. The potential for flash floods to occur on a synoptic scale underscores the need for international collaboration to mitigate the risk of these disasters. By pooling resources and expertise across nations, it is possible to develop strategies that reduce the impact of flash floods and enhance preparedness for future events.

Pool risk diversification amongst nations can promote sustainable land use practices and investments in more resilient infrastructure. For example, suppose multiple countries pool their resources to create a fund covering losses from extreme precipitation events. In that case, they may be more likely to invest in climate adaptation measures such as flood protection infrastructure, early warning systems, and disaster risk reduction programs. Pool risk diversification amongst participating nations promotes cooperation and helps reduce insurance costs. By pooling resources and spreading the risk, insurance providers can offer more competitive rates to more countries, making it more affordable for nations to protect themselves against extreme weather events. The cost of extreme weather events can have devastating consequences on the economies and livelihoods of vulnerable countries. However, insurance solutions can help protect countries against the financial impacts in the context of a changing climate.

In this context, the Sendai Framework for Disaster Risk Reduction was established in 2015. It is a 15-year voluntary, non-binding agreement aimed at reducing disaster risk by preventing new risks and mitigating existing ones. It establishes that investing in disaster risk reduction can substantially benefit sustainable development, including increased resilience to climate change and its impacts. The Sendai Framework also emphasizes the need to enhance access to financial protection for disaster-prone countries, particularly developing countries, including access to insurance and other financial instruments. The Sendai Framework aims to significantly improve global collaboration with developing countries by providing appropriate and sustainable assistance that complements their domestic efforts in implementing the current framework by 2030 (United Nations, 2015). The 2015 COP agreement established in Paris aligns with the Sendai Framework by recognizing the need for various financial instruments and tools to support the transition to a low-carbon, climate-resilient economy. Article 8 of the Paris Agreement (United Nations Framework Convention on Climate Change, 2015, p. 12) explicitly mentions that the parties acknowledge the significance of preventing, reducing, and managing the loss and damage caused by the negative impacts of climate change, including extreme weather events. This includes "risk insurance facilities, climate risk pooling, and other insurance solutions" (United Nations Framework Convention on Climate Change, 2015, p. 12) particularly for developing countries.

Following the 2015 Paris Agreement and the Sendai Framework, the G20 and V20 countries created the InsuResilience Global Partnership in 2017. InsuResilience Global Partnership aims to make insurance and other risk transfer mechanisms more available to vulnerable people and countries. InsuResilience Global Partnership (United Nations, 2019) brings together governments, the private sector, civil society, international organizations, and academia to improve disaster and climate resilience by providing financial protection to those most in need. According to the InsuResilience Global Partnership launch document (United Nations, 2019), it has two aims.

- To assist countries so they can effectively respond to the consequences of climate change, especially in the aftermath of a disaster (ex-post dimension).
- To provide support to countries so they can prepare for natural disasters by utilizing pre-planned climate and disaster risk financing and risk transfer solutions, such as insurance (ex-ante dimension).

Despite the creation of the Sendai Framework for Disaster Risk Reduction and the InsuResilience Global Partnership, we need to improve existing solutions, develop new ones, perform further research on climate risk, and strengthen international collaboration. All this effort is required to protect vulnerable countries financially. In this context, this thesis contributes to the discussion by analyzing the effectiveness and feasibility of risk pooling as a tool for climate risk transfer in developing countries. By examining empirical rainfall data, we seek to uncover the potential benefits and limitations of international risk pooling against excessive precipitation and to study the role that risk pooling plays in enhancing developing countries' resilience to the impacts of climate change.

Assessing risk due to extreme precipitation requires an integral multidisciplinary perspective, as the problem, on the one hand, is that extreme rainfall is a natural phenomenon that has always occurred in the Earth's atmosphere. On the other hand, extreme rainfall poses dangers to societies. For example, the IPCC (2022a) emphasizes finances' crucial role in adaptation and resilience as a key factor in facilitating climate risk management. Although the private sector represented 0.05% of total climate finance and 1% of adaptation finance in 2018, the promotion from this sector for adaptation has grown progressively. Ciullo et al. (2023) remarks that global pooling among countries is designed, in principle, to spread their risk and reduce their contribution. The authors found that financial instruments established in advance increase economic resilience by ensuring a consistent funding stream in the aftermath of disasters. This enables governments to distribute costs over a predictable timeframe.

Flash floods and disaster occurrences have unique local characteristics that need to be recognized to determine the best course of action for reducing disaster risk, regardless of the drivers of local, national, regional, or global (United

Nations, 2015). Factors such as the local topography, soil conditions, and infrastructure can all play a role in determining whether or not the rainfall in a given area is "excessive". Despite these complexities, establishing a clear and consistent threshold for excessive rainfall is crucial to assess risk effectively. For this thesis, it was necessary to examine the diverse approaches that various institutions and researchers use to establish a threshold for what constitutes an excessive rainfall event.

Panda and Surminski (2020) emphasizes that the lack of data on impacts creates the necessity for monitoring and evaluating resilience development made possible by international platforms or projects. They mention that new data and methods are needed to track resilience improvement through these activities. Creating a database of flash floods coupled with damage data becomes a priority.

The first step to reduce flash flood risk diversification is identifying and quantifying public contingent liabilities. Understanding the actual costs of natural hazards requires a well-maintained database of hazard impacts and the related economic implications, as well as a mechanism to track and report on post-disaster expenditures (Justiniano et al., 2021). Once the physical characteristics of flash floods and the threshold of excessive rain are established, the next step is to merge with impact data. It is crucial to assess the actual costs of high flash flood risk, and this matter is growing as climate change consequences are more conspicuous (United Nations Office for Disaster Risk Reduction, 2022).

This thesis aims to contribute to the initial stages of flash flood risk diversification efforts for both individual nations and the international community as a whole. The central question we aim to address is: What are the global patterns, characteristics, and economic impacts of flash floods? By focusing on analyzing flash flood events and their associated rainfall patterns, we seek to provide valuable insights that can inform targeted risk reduction strategies. Through this research, we aim to enhance the understanding of the factors contributing to flash floods, thereby enabling policymakers and disaster management authorities to make informed decisions to reduce communities' vulnerability to these natural disasters. Our ultimate goal is to contribute to a more resilient and prepared global community facing flash flood risks.

1.1 Disaster Databases

The development and maintenance of global flood databases represent a monumental task that only a handful of institutions can undertake. The number of comprehensive global flood databases remains limited, constraining the availability of crucial information for understanding and mitigating flood risks on a global scale.

Nevertheless, there exist examples of initiatives that are dedicated to providing updated flood-related news and information from across the globe. One example is FloodList, which is managed by a committed team focused on delivering the latest updates on flood events worldwide. FloodList is financially supported by Copernicus, the European Union's program for monitoring the Earth's environment through satellite and in-situ observations (The Floodlist Team, 2023). Another notable initiative is the European Flood Awareness System (EFAS), which aims to facilitate preparatory measures ahead of major flood events, especially in large trans-national river basins and across Europe. EFAS is the first operational European system for monitoring and forecasting floods globally. It has been fully operational as part of the Copernicus Emergency Management Service (EMS) since 2012 (European Flood Awareness System, 2023).

Dartmouth Flood Observatory

Dr. Robert Brakenridge heads the Dartmouth Flood Observatory (DFO) at the University of Colorado in Boulder. The DFO produces up-to-date maps of global flooding events. In an interview done with Science Insider (2023) Brakenridge stated, that he established the lab in 1993, and that uses satellite images to track water level changes. His lab is also exploring other techniques, such as the use of microwave sensors based on satellites, to monitor river levels. According to Brakenridge (2023) the mission of Dartmouth Flood Observatory is to obtain and conserve a digital map archive of the alterations in Earth's surface water, for public use.

Darthmouth Flood Observatory (2023) users can explore the latest flood maps, download historical datasets, and access a range of other tools and resources for monitoring and analyzing flood events worldwide. It should be taken into account that "data are poor or missing in the early-mid 1990s" (Dilley, 2005, p 29) and to a degree, it extends to the 2000s. The discrepancy in the number of flood events is illustrated by Table 1.1. These databases report disasters as "floods". In general, during the years 2000 to 2018, the number of flood incidents in DFO and EM-DAT showed a positive timeseries correlation (Pearson correlation $r = 0.591$, $P < 0.01$) (Tellman et al., 2021).

Thus DFO has been used in the Global Flood Database project as a joint effort between Cloud to Street and DFO, funded by Google Earth Outreach. The researchers participating in this project have affiliations with several institu-

Table 1.1: World databases for Floods.

Name	Number of Events	Period	Sources
Dartmouth Flood Observatory	5130	1985 - 2021	News
EM-DAT	8500	1985 - 2022	News

tions, including the Columbia Earth Institute, University of Arizona, University of Michigan, University of Texas at Austin, University of Colorado Boulder, INSTAAR, University of Washington, Google, and Science Systems & Applications Inc./Biospheric Sciences Lab at NASA Goddard Space Flight Center (The Global Flood Database, 2022).

Emergency Events Database

The Emergency Events Database (EM-DAT) is a comprehensive database managed by the Centre for Research on the Epidemiology of Disasters (CRED), created by the World Health Organisation and the Belgium Government. The database is a reference source on natural disasters, technological disasters, and complex emergencies that have occurred worldwide. EM-DAT records data on natural disasters that have caused significant impacts, such as loss of life, damage to infrastructure, and displacement of populations. The database provides information on the number of people affected by natural disasters, the economic cost of these events, and the response efforts implemented to mitigate their effects. It enhanced the compilation of disaster events, a tendency that started growing with the Office of Foreign Disaster Assistance (OFDA) as shown in Figure 1.3.

EM-DAT has served as a primary reference for disaster-related information in numerous scholarly articles and publications. While it is not without its limitations, EM-DAT remains an invaluable resource for researchers and policymakers alike. Its comprehensive database of disasters provides crucial insights into the frequency, impact, and distribution of various types of disasters, including floods. Despite any shortcomings, EM-DAT continues to be an essential tool in our efforts to understand, mitigate, and respond to disasters worldwide.

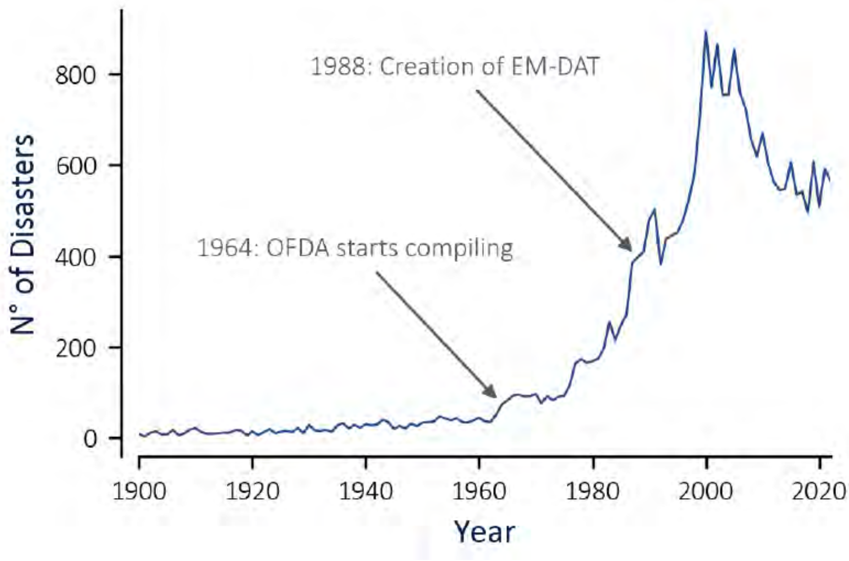

Figure 1.3: Plot Number of Worldwide Disaster Registration per Year. Source: Centre for Research on the Epidemiology of Disasters (CRED) and Institute of Health & Society (IRSS) (CRED and IRSS, 2023).

Chapter 2

Methodology

This chapter focuses on the collection and analysis of event and rainfall data to understand the occurrence and impact of flash floods. It outlines the methodology used in this thesis. Our approach involves several key steps, beginning with the selection of relevant flash flood events from the EM-DAT database.

2.1 Event and Rainfall Data

The first step in analyzing flash flood events is utilizing our chosen database and geo-locating its entries for accurate assessment. This EM-DAT database, serves as a valuable resource due to its extensive coverage of historical disasters, including flash floods, from around the world. By leveraging this dataset, the study aims to establish an understanding of the distribution and frequency of flash floods across different geographic locations. For the precipitation data, we used the Integrated Multi-satellitE Retrievals for Global Precipitation Measurement (IMERG).

2.1.1 Flash Flood Events and Geo-Locations

We choose to work with the EM-DAT database to create a subset only containing *flash floods* events. These events must include a defined start and end date. We are aware that also *riverine floods* may be caused by excessive rainfall; nonetheless, they can originate from snow-melt or different sources different from rain, and for this reason, they are not considered. Moreover, we decided to use the definition of subtype flash flood in EM-DAT (2023):

"Flash flood: Heavy or excessive rainfall in a short time that produces immediate runoff, creating flooding conditions within minutes or a few hours during or after the rainfall."

Other filters were applied to further narrow down the data. For example, we decided to leave any event that lacked two administration levels for location

(Figure 2.1). The locations are pinpointed either to the state/province/canton or city, thus restricting the area where the event occurred. So it was essential for each identified event to have:

1. A clearly reported *Start and End Date*,
2. and an identifiable name at the sub-country level.

Once filtered the EM-DAT database contained the minimum requirements, the next task was to couple a latitude and longitude corresponding to each city/point. As outlined in Figure 2.1, we used a Python package from GeoPy Contributors (2018), which enables the user to input a city name and from OpenStreetMaps (OpenStreetMap Foundation, 2023) extract geo-referenced position. This allowed us to continue to the next step.

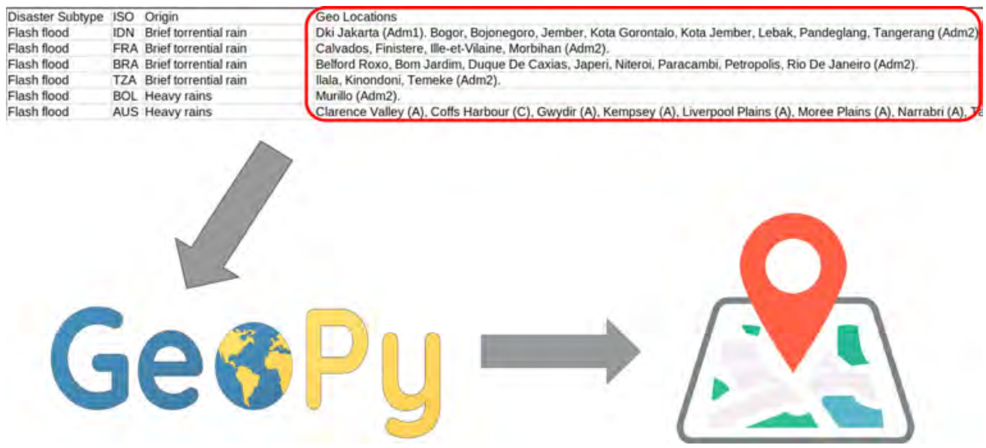

Figure 2.1: Geolocation Process Outline.

To assess the risk of excessive rain events amongst different countries, it is essential to first access and analyze precipitation data from various sources. A precipitation database is a collection of historical and real-time precipitation data, which is used to understand patterns and trends in precipitation over time. It can be collected from a variety of sources, including ground-based weather stations, satellite observations, and radar systems. Once collected, the data can be analyzed to identify patterns and trends in precipitation.

2.1.2 Integrated Multi-satellitE Retrievals for Global Precipitation Measurement (IMERG)

The Tropical Rainfall Measurement Mission (TRMM) is a precursor the Global Precipitation Measurement (GPM) mission, which includes the Integrated Multi-satellitE Retrievals for GPM (IMERG) product. TRMM was launched in 1997 as a joint mission between NASA and the Japan Aerospace Exploration Agency (JAXA) to study tropical rainfall (NASA, 2023). The success of TRMM demonstrated the importance of satellite-based precipitation measurements and paved the way for the development of the GPM mission, which aims to provide global precipitation measurements with greater accuracy and coverage.

IMERG is a dataset produced by NASA that provides estimates of precipitation and combines the data from all of the satellites in the GPM constellation, as well as other satellites that provide precipitation data and ground base stations. The product is updated every half-hour and provides estimates of precipitation intensity and accumulation at a high spatial resolution of $0.1 \times 0.1°$ (≈ 11 km). Gautam and Pandey (2022) did a validation with groundstations in some points of India and concluded that precipitation estimates provided by IMERG are the newest and most advanced products of their kind, and they have been shown to outperform the previous generation of precipitation data products, which were produced by TRMM.

A cloud-based platform is used to access and manage the IMERG rainfall database. They allow users to access software applications and computing resources without expensive hardware or software installations. Users with an internet connection can access the platform from anywhere, making them ideal for remote work and collaboration. Cloud-based platforms such as Google Earth Engine and Microsoft Planetary Computer are software platforms that offer access to large amounts of geospatial data. These are therefore the tools being used in this thesis.

Overall, Microsoft Open Source et al. (2022) provides users with a powerful set of tools and services for working with geospatial data in the cloud. The platform's focus on sustainability and environmental stewardship makes it an attractive option for organizations and individuals who are interested in using technology to support more sustainable practices and protect the natural environment.

2.2 Coupling EM-DAT Flash Floods with IMERG

Once the EM-DAT database was filtered and georeferenced, the next step was to identify each event in the IMERG database. The *nearest neighbor* method was used to find each flash flood corresponding to the latitudes and longitudes obtained through the process explained in Section 2.1.1. During the extraction, a buffer of three days before was added to the reported date.

2.2.1 Excessive Precipitation Thresholds

Choosing the threshold for extreme precipitation events is critical for the design and maintenance of infrastructure such as buildings, roads, bridges, and dams. The design of infrastructure must take into account the expected maximum precipitation and the intensity of the rainfall, as well as the duration of the event. If the threshold for an extreme precipitation event is set too low, the infrastructure may be insufficiently designed to withstand the forces of the event, leading to damage or failure.

Insurance companies and risk managers need to establish thresholds for extreme precipitation events to determine the likelihood and severity of losses. The threshold is an essential factor in determining the insurance premiums and risk management policies for different regions and contexts. Insurers need to consider the potential for extreme precipitation events when assessing the risks of insuring a property or a region. If the threshold for an extreme precipitation event is low, insurers may be exposed to higher risks of losses, leading to higher premiums. On the other hand, if the threshold is set too high, the insurance premiums may be unnecessarily high, leading to an under-insurance problem where people and businesses are not adequately insured.

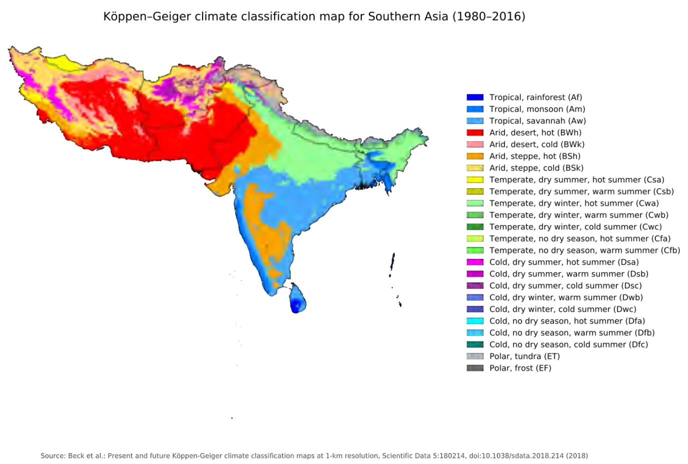

Figure 2.2: Köppen-Giger Climate Classification map of South Asia. Source of Map: Beck et al. (2018).

The appropriate threshold for an excessive precipitation event must consider various factors, including the location, duration, and intensity of the event, as well as the potential risks and vulnerabilities of the area. The first threshold is emulating the India Meteorological Department (2022), who have marked excessive precipitation as any precipitation that surpasses the daily accumulative rainfall in the 60th quantile. This is mainly because India is a microcosmos of the world as it is a megadiverse country. Given its geographical position in the world and the Himalayan Mountains, India poses different climate classifications from tropical wet to arid and mountainous climate, this is shown in Figure 2.2. Moreover, this threshold is currently in operational use and also by Liang et al. (2019), who studies flood hazards in China.

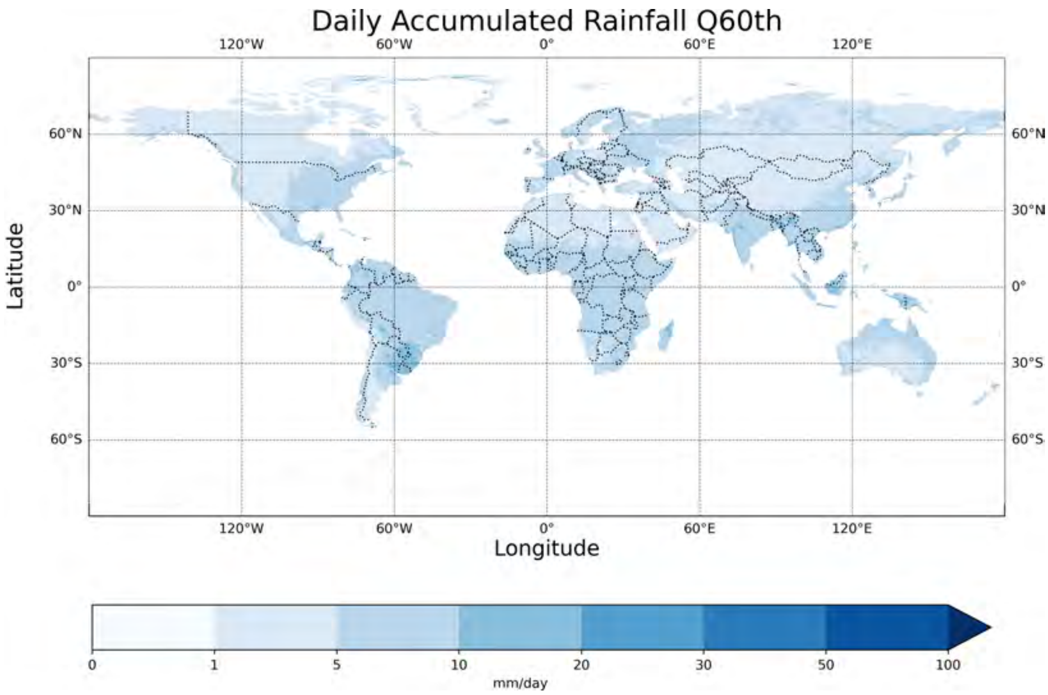

Figure 2.3: Daily Accumulated Rainfall q_{60}, or the 2001 - 2020 Period.

It can be observed in Figure 2.3, that excluding parts of Greenland and Antarctica, the daily accumulative rainfall q_{60} overland is above 1 mm/day according to IMERG period (2001 - 2020). Large portions of the globe are between 1 - 5 mm/day, and 5 - 10mm/day. To a lesser extent but noticeable are the areas where the daily accumulative rainfall q_{60} surpasses 10mm/day, such as the region between Paraguay, Brazil, Argentina, and Uruguay, Northeast Madagascar. Some areas surpass the 10mm/day mark, particularly in Southeast Asia Indonesia, Brunei, Papua New Guinea, the western coast of India, and the border region with Bangladesh and Myanmar.

Once the time series that resulted from coupling EM-DAT with IMERG (Section 2.2) the next step is to make sure that indeed it was a rainfall-related event. Then we filter the extracted points using the daily accumulative rainfall q_{60}, as a minimum requirement for excessive rainfall.

2.2.2 Indices

For a metric to represent extreme flash floods, the daily accumulative rainfall q_{90} was used. The extension of the amount millimeters that is the threshold goes from a minimum in the Mongolian Gobi Desert of 5.7 mm/day and a maximum in India of 60.0 mm/day. In Figure 2.4, rain patterns are truly diverse and the impact of flash floods depends on many factors. The main factor is the amount of rain that falls in a flash flood relative to the local normality. Human settlements adapt their hydrological infrastructure to handle typical amounts of precipitation, meaning that in absolute terms 10 mm/day may not provoke a disaster in India but will be an extreme event in the Mongolian Gobi Desert.

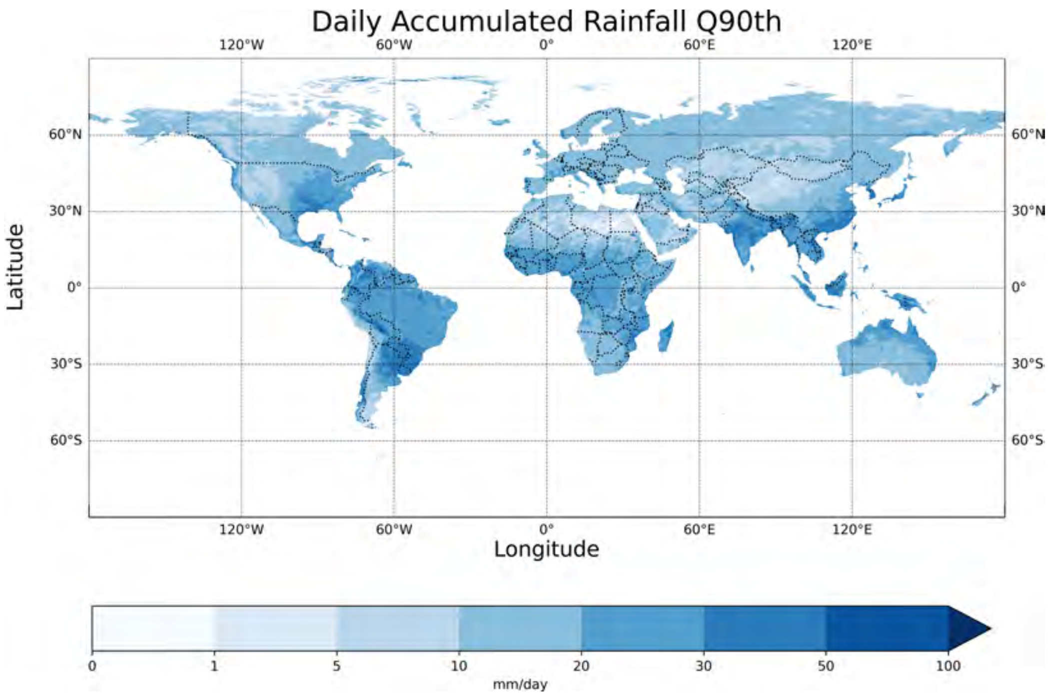

Figure 2.4: Daily Accumulated Rainfall q_{90}, or the 2001 - 2020 Period.

For this reason, it became conspicuous that we would benefit during the analysis of flash floods from contextualizing to local terms the amount of rainfall using the daily accumulative rainfall q_{90}. By accounting for local variations, q_{90} provides a more nuanced understanding of how different regions respond to rainfall, allowing for more accurate assessments of the flash flood. This localized approach improves the precision of our analysis. Allowing the development of Accumulative Rainfall Relative Index (ARRI) in Equation 2.1.

$$Accumulative\ Rainfall\ Relative\ Index = \frac{MeanSum_i}{Mean\ Daily\ q_{90_i}} \tag{2.1}$$

ARRI is in terms of the Mean Sum from the reported flash in EM-DAT divided by the Mean Daily Accumulative Rainfall q_{90} of that flash flood. This index is a localized measure of the amount of rainfall.

$$Intense\ Relative\ Rainfall\ Index = \frac{Mean\ MaxInt_i}{Mean\ Daily\ q_{90_i}} \tag{2.2}$$

At the same time, it is useful to see how much that daily accumulative rainfall q_{90} fell during the maximum peak of intensity during the reported flash flood. Another index was proposed but focused on localizing the maximum intensity of the flash flood. Equation 2.2 is a measure of how much of the Mean Daily Accumulative Rainfall q_{90} at the Mean Maximum Intensity Rainfall.

2.2.3 Regional Division

For a complementary analysis, a regional approach to countries was taken. The countries were separated among 10 regions, principally on geographic proximity, and similarities in rain patterns. Where in the case of Latin America, for similarities in the reporting behavior in EM-DAT. In Figure 2.5 the world is divided into: Oceania, Southeast Asia, Central Asia and Georgia, East Africa, West Africa, the Mediterranean Basin, Latin America, and the merging of the United States of America with Canada.

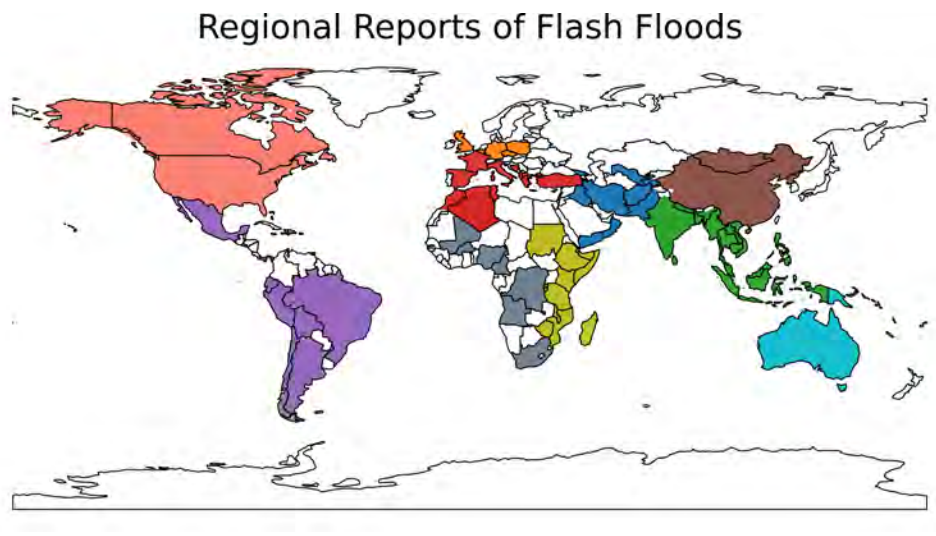

Figure 2.5: The Regional Division of Countries with Registered Flash Floods.

Overall, our methodology integrates data from IMERG precipitation database and employs specialized techniques to analyze the complex interactions between flash floods, their localized characteristics, and their impacts.

Chapter 3

Results and Discussion

3.1 Results

In this section, we present the results of our analysis of flash flood events. We begin by examining the remaining flash floods after quality control and their spatial and temporal distribution, highlighting regions with high frequency and severity.

3.1.1 Flash Flood Events after Quality Control

Figure 3.1 are the punctual flash floods remaining after the quality control done on the flash floods database in EM-DAT (2001 - 2020). Although there are events on every continent, events are more numerous in India and Southeast Asia. Starting from a total of **1002**, 834 are left of which 302 with reported damages in USD.

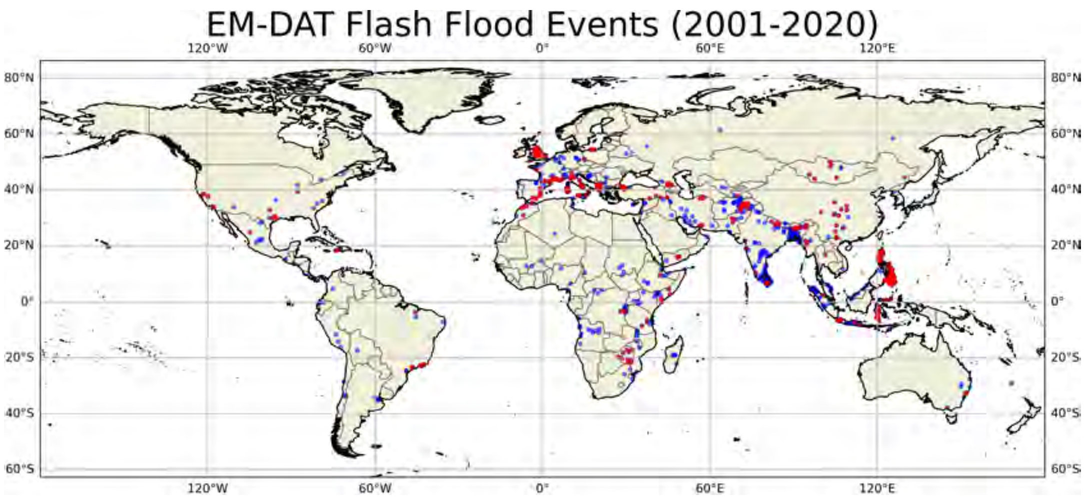

Figure 3.1: Specific location for a total of 834 flash floods, 302 with reported damages in USD.

Figure 3.2 shows a distribution of flash floods worldwide. However, a bias exists to the east of the Greenwich Meridian, particularly in the European Mediterranean, Pakistan, Afghanistan, India, and Southeast Asia. In the Americas, flash floods occur less or are reported less in EM-DAT (2001 - 2020). Moreover, the most intense and with the highest amount of rainfall are in Central South and Southeast Asia. Also, the Mediterranean has intense and large amounts of rain. To a lesser extent, this holds for East Africa, the coast of Angola, and the People's Republic of Congo. Isolated flash floods occurred on the southeast coast of Brazil, and Argentina. Regarding the relatively small and low-intensity rainfalls distributed along the Sahel, Sahara, mainland Russia, the Mongolian Gobi Desert, Peru, Northern Brazil, Australia, China, and the United States of America.

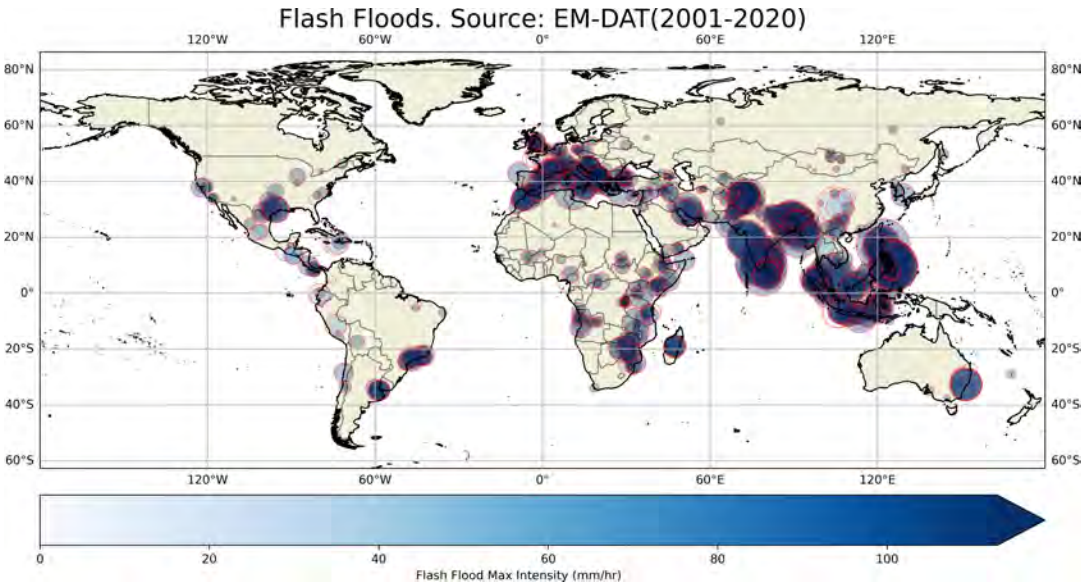

Figure 3.2: Specific location for all flash floods. Being the radius proportional to the total sum of rainfall and the shades of blue are the maximum intensity of the event.

EM-DAT has one entry per flash flood independently if they occur in one or more points, are ensemble back together, and in Figure 3.3 are counted by country. As the individual points from Figure 3.1 are compiled in the counts per country, a worldwide distribution also exists. However, the countries that experience more flash floods are Central and Southeast Asia. The five most affected countries by flash floods are Indonesia (29), the Philippines (26), Pakistan (14), Afghanistan (12), and India (12), as shown in Table 3.1. On the otherside of the spectrum, there are countries such as Colombia, Kazakhstan, Russia, among others that did register an event that surpassed individually the daily accumulative q_{60} however, not in the compound event. Thus doesn't appear in any shade of green in Figure 3.3.

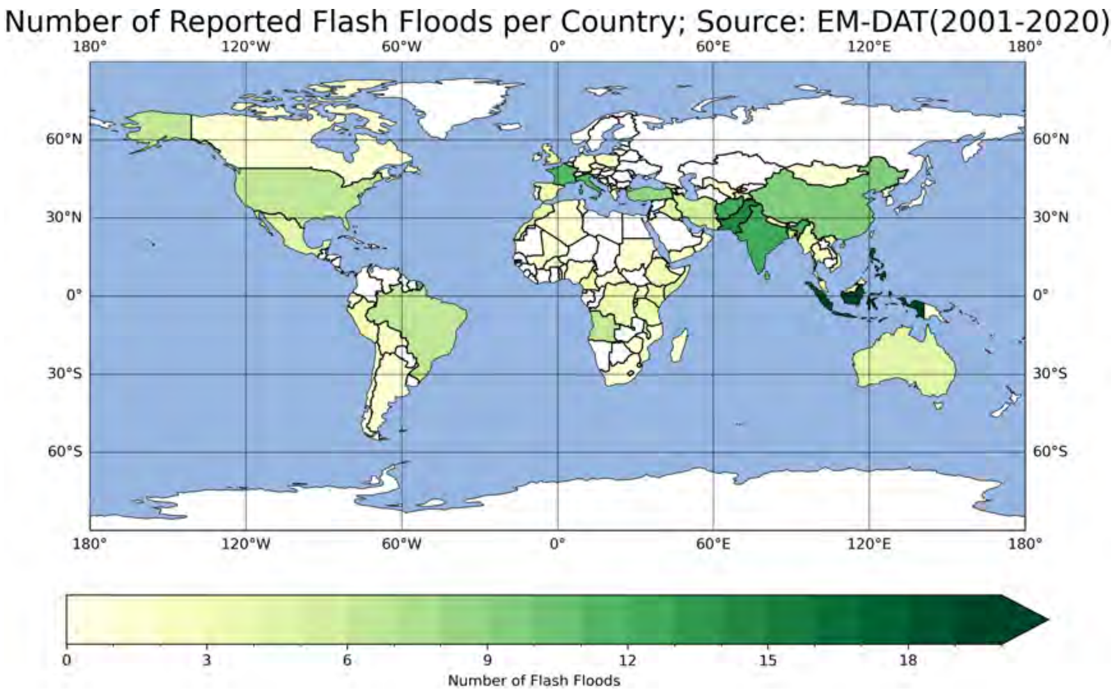

Figure 3.3: Number of Reported Flash Floods in EM-DAT per Country during the years 2001 - 2020.

Table 3.1: Top five countries in the number of flash floods period (2001 - 2020).

Country	IDN	PHL	PAK	AFG	IND
Flash Floods	29	26	14	12	12

Case Study: Pakistan

A representative illustration encapsulating an entry in EM-DAT is the case of the Pakistan flash flood in 2010. Documented in EM-DAT from July 28th to August 7th, 2010, spanning nine days, this entry reveals a staggering impact. It reports 20,356,550 people affected and records 1985 fatalities during the specified time frame. Regarding the economic damages reported in EM-DAT, total damage of 12,750,062 USD, only 134,211 USD of those were insured. This amount was adjusted to 2019.

Figure 3.4 a) illustrates the accumulated rainfall from July 28th to August 7th of 2010 represented in shades of blue. Values of accumulated precipitation start after 25mm and it is visible that it covers roughly 2/3 of The Islamic Republic of Pakistan. However, the largest accumulated precipitation values are concentrated in the country's north. In this region, there are values from 150 to 300mm that cover a large portion of this part of the country, with some spots that even surpass 400mm. The shades of purple in Figure 3.4 b) represent the values extracted from CLIMADA LitPOP exposure in USD. The concentration of wealth in Figure 3.4 b) follows the distribution of population centers, from Peshawar, Islamabad, Lahore, and all the way south to the coast where Karachi. For both maps of Pakistan, the red dots are the points affected by the flash flood of 2010 according to EM-DAT, and that were geolocated by GeoPy.

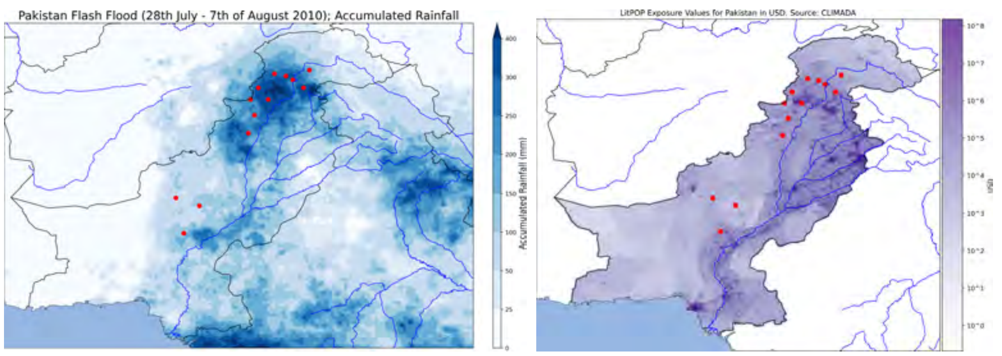

a) b)

Figure 3.4: Figure a) is the rainfall accumulated during the flash flood of 2010 registered in EM-DAT and Figure b) represents the values extracted from CLIMADA LitPOP exposure in USD.

3.1.2 Regional Analysis

The regions divided in Table 3.2 show Southeast Asia is the most prone to flash floods, registering an alarming 95 incidents, making it the region with the highest frequency. Followed by the Mediterranean Basin region, Central South Asia, and Georgia, both tied with 45 occurrences. In the fourth position, East Africa has experienced 28 flash floods, while Latin America has the fifth spot with 25 recorded incidents. West Africa 16 flash floods, East Asia, comprises only 11 counts of occurrences, Northern Europe, U.S.A & Canada, and Oceania all in single digits.

Table 3.2: Number of flash floods per region; period (2001 - 2020).

Region	Flash Floods
Southeast Asia	95
Central South Asia & Geo	45
Mediterranean	45
East Africa	28
Latin America	25
West Africa	16
East Asia	11
Northern Europe	8
U.S.A. & Canada	7
Oceania	5

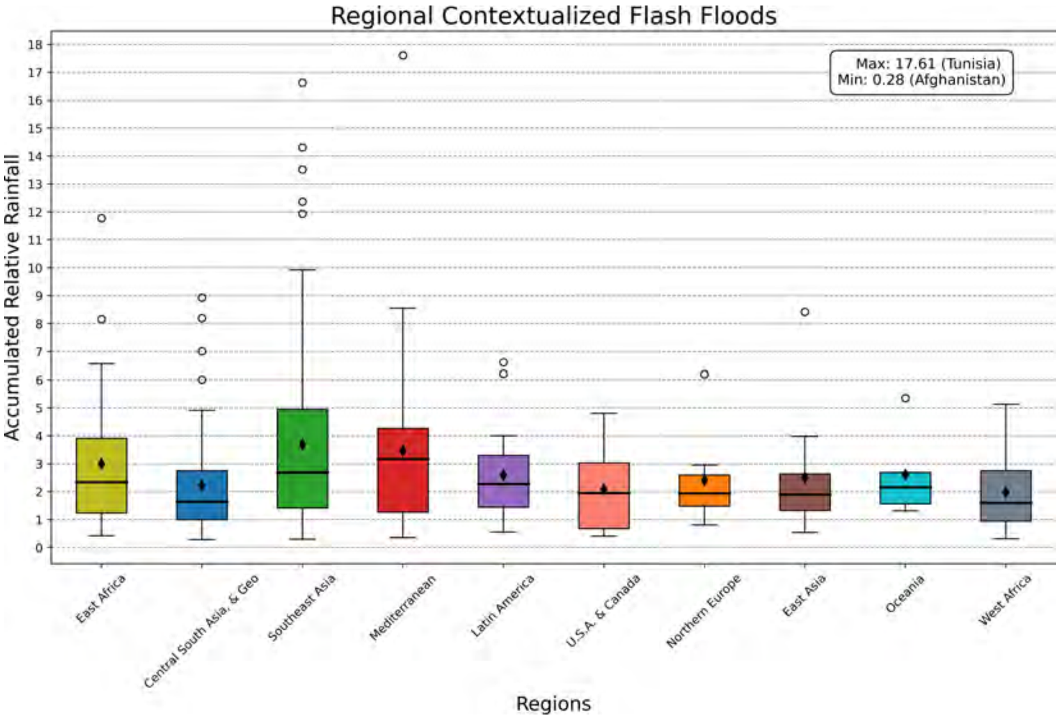

Figure 3.5: Boxplots depicting regional flash floods against the Accumulative Relative Rainfall Index.

The plot in Figure 3.5 illustrates the behavior of flash floods concerning the Accumulative Relative Rainfall Index (ARRI) after being divided in a regional context. The maximum value of ARRI occurred in the Mediterranean region, Tunisia where it rained 17.61 times the q_{90} daily accumulated. Despite this, the region with the largest values of ARRI is Southeast Asia, followed by the Mediterranean. In contrast, the minimum value of ARRI happened in the Central South Asia & Georgia region, Afghanistan. Most regions have their lowest values $ARRI \leq 1$, meanwhile, all regions have the mean $ARRI \approx 2$ or above. However, the median in all cases is smaller than the mean. All regions have local outliers except West Africa and the combination of the United States of America and Canada.

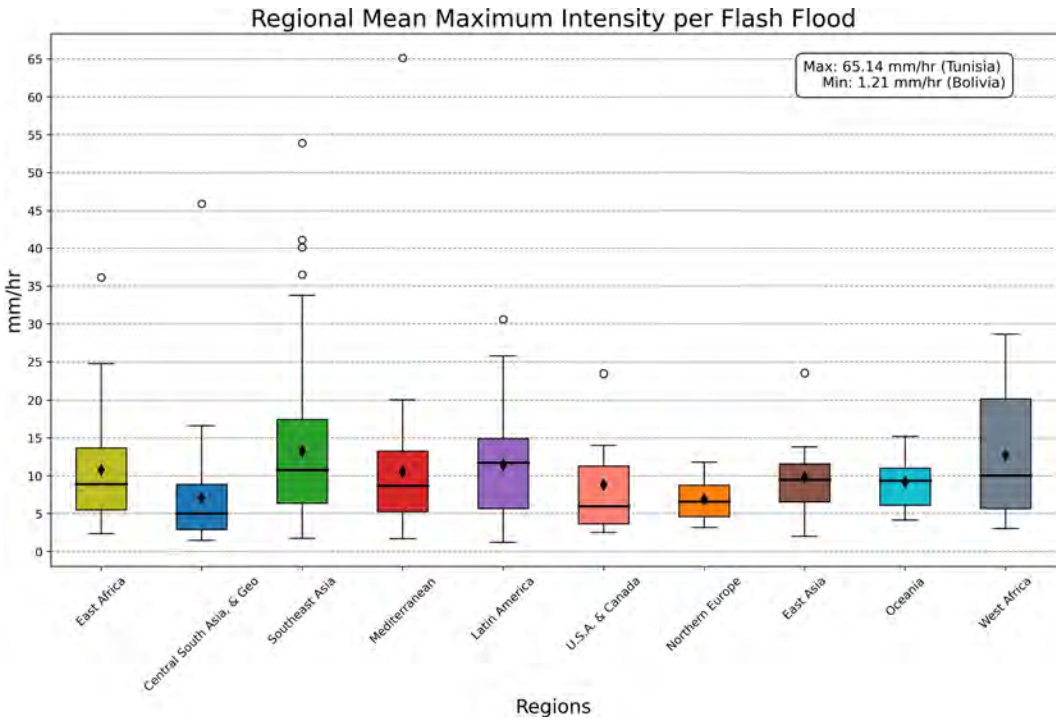

Figure 3.6: Regional boxplots in terms of Mean Maximum Intensity per Flash Flood.

In this case, the mean maximum intensity is a measure of the most amount of rain that fell in one hour during the flash flood. The intensities of the flash floods vary per region as shown in Figure 3.6. The largest value of the mean maximum intensity during an event occurred in Tunisia with an impressive amount of 65 mm in one hour, succeded by a flash flood in Southeast Asia and Central South Asia & Georgia. In contrast, a flash flood in Bolivia had a mean maximum of 1.21 mm/hr, being the lowest registered. All region means surpass 5mm/hr, this also holds for the median. Both Southeast Asia and Latin America have means and median between 10 to 15 mm/hr, whereas the rest have one or both of these values below 10 mm/hr.

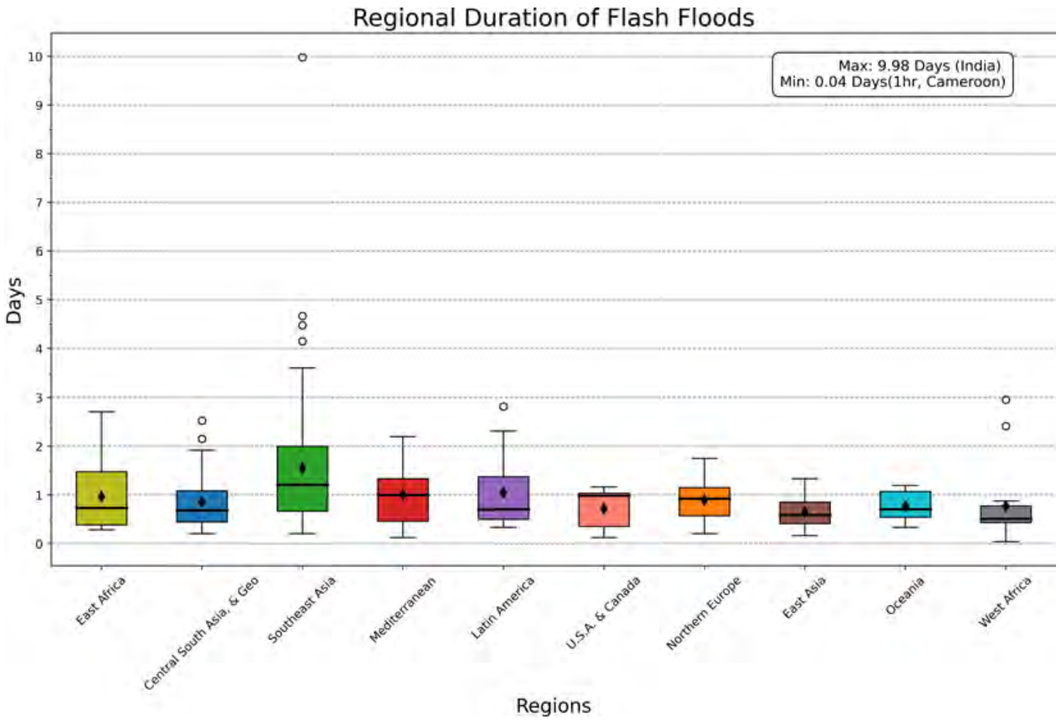

Figure 3.7: Regional boxplots in terms of Mean duration per Flash Flood.

In terms of the duration of the flash floods registered in EM-DAT most of them had a median under 1 day. Although the mean is higher than the median this holds in most cases, with the noticeable exception being Southeast Asia. As illustrated in Figure 3.7 the flash flood that lasted the most was Southeast Asia with an event of 9.98 days in India. The shortest flash flood lasted only one hour, which happened in Cameroon.

3.1.3 Cost Analysis of Flash Floods

The distribution of intensity and accumulative precipitation can be observed in Figure 3.8. These flash floods are the ones that caused reported damages in the EM-DAT database. It is skewed to Europe, the Republic of Türkiye, Zimbabwe, Southeast Asia, and Pakistan. A cluster of events in the United States of America, Brazil, China, and Australia. The remaining flash flood occurrences as sparse, with a noticeable occurrence in Haiti.

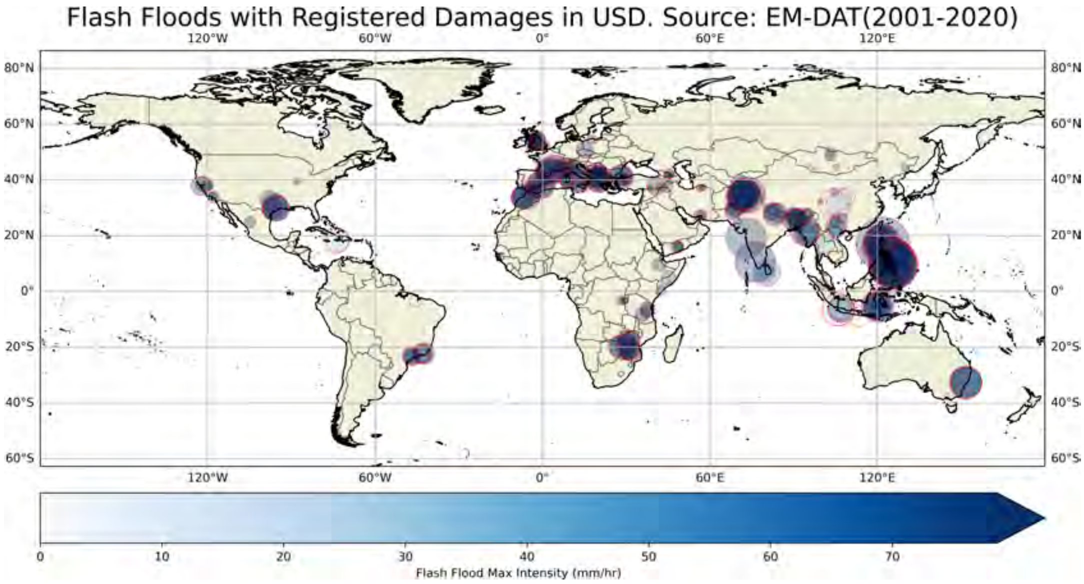

Figure 3.8: Flash Floods with Registered Damages in EM-DAT during the years 2001 - 2020.

The events showcased in Figure 3.8 have been consolidated into individual entries within the EM-DAT database. Figure 3.9 provides an overview of the aggregated impact of flash floods at the national level. Pakistan emerges as the most heavily affected country, leading the tally with damages exceeding 8 billion USD, trailed by France, China, India, and the United States of America, in that order. Other nations have been comparatively less affected.

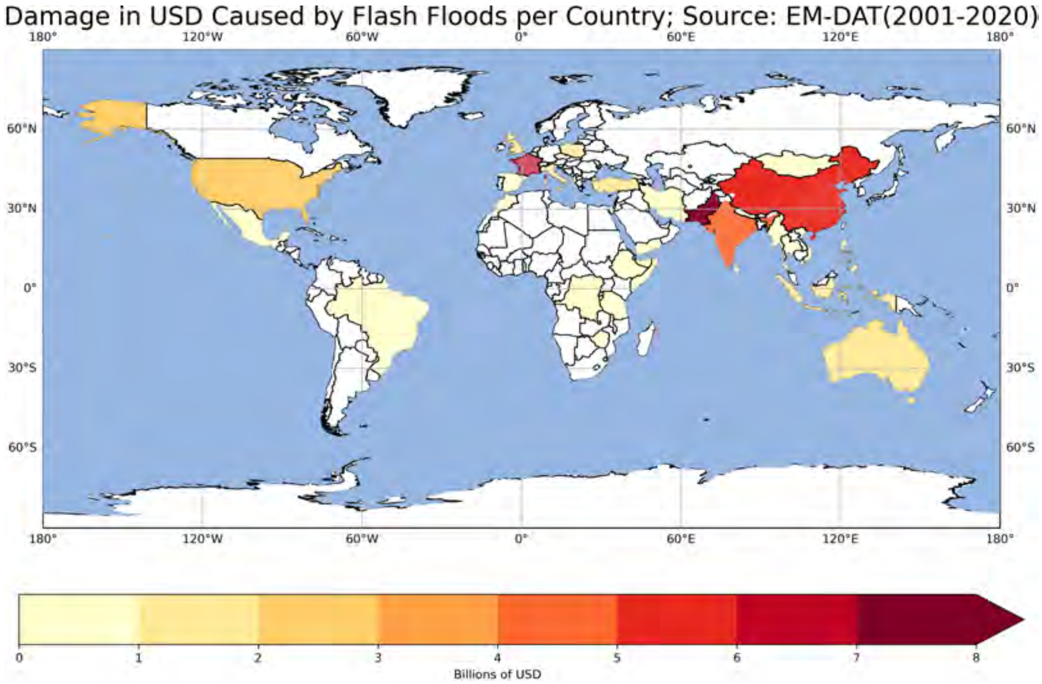

Figure 3.9: Aggregate damage in U.S. Dollars from Flash Floods.

Damage Function

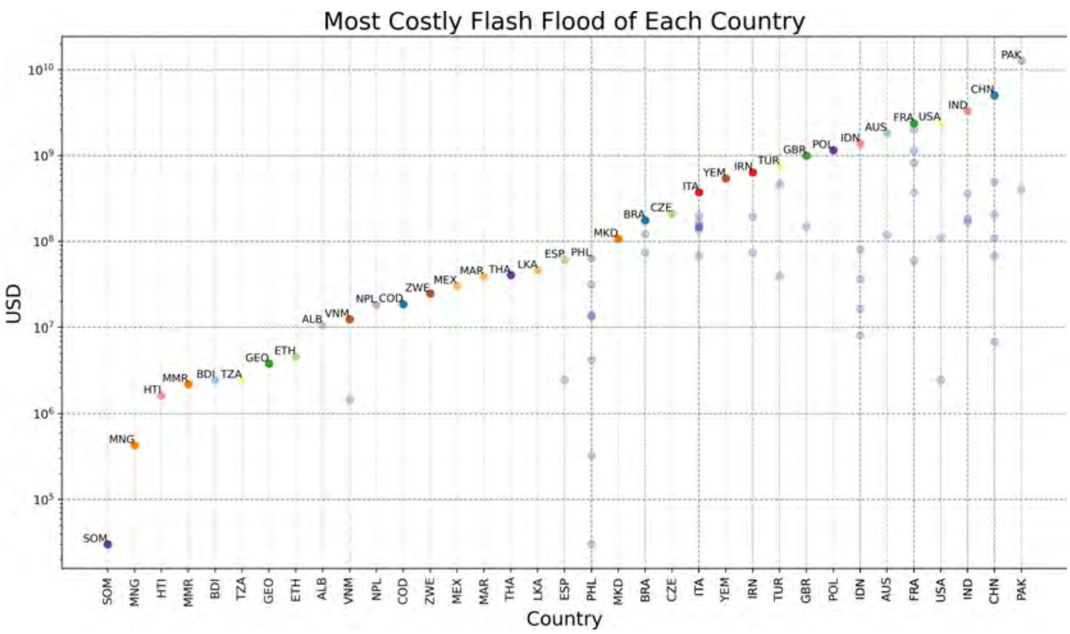

Figure 3.10: Flash Floods Plotted by Country and Damages in USD.

In Figure 3.10, the most costly flash floods reported in EM-DAT of every country are sorted in damage in USD. Somalia with one flash flood damaging in the range of 10^4 USD, Mongolia with one flash flood damaging 10^5 USD. Meanwhile, the rest of the nations all have their most costly flash flood greater than 10^6 USD, with the top five most costly events occurring in Pakistan (over in billion USD, 10^{10} USD), China, India, the United States of America, and France (all with damages in 10^9 USD range).

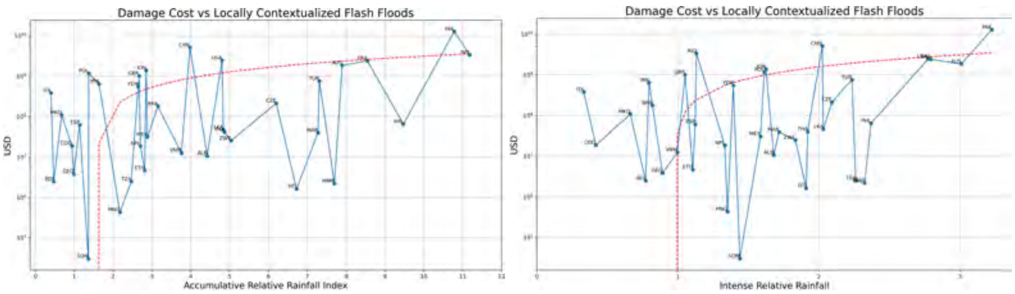

a) b)

Figure 3.11: Both Figures are the Damage Cost vs Locally Contextualized Flash Floods. Y-axis is a logarithmic scale of USD with the red dotted line is the linear tendency. Figure a) is the Accumulative Relative Rainfall Index and Figure b) is the Intense Relative Rainfall Index.

Only the most costly events from each country were plotted in Figures 3.11 a) and 3.11 b), the Y-axis is USD in a logarithmic scale starting from 10^4 to a little more than 10^{10}. The X-axis for Figure 3.11 a) is in terms of the Accumulative Relative Rainfall Index (Equation 2.1), only four flash floods did not equal or surpass this index, which means that the majority of the flash floods accumulated more than the relative daily q_{90}. On the other hand, in Figure 3.11 b) the X-axis is in terms of Intense Relative Rainfall Index (Equation 2.2), which is a measure of maximum intensity relative to the q_{90} daily accumulative rainfall. A total of six flash floods are under IRRI $= 1$, subsequent events that are equal to or greater than 1 are twenty-nine occurrences. The five most intense rainfalls occurred in Pakistan, Australia, France, the United States of America, and the Philippines. All previously mentioned flash floods surpass the two times the index. Moreover, Australia and the Philippines surpass by three their daily accumulated q_{90} in one hour respectively.

$$Damage\ Function = a_1 e^{b_1 \cdot ARRI} + a_2 e^{b_2 \cdot IRRI} \tag{3.1}$$

Using the exponential relationship between ARRI, and IRRI with damages represented in USD, Equation 3.1 is proposed. Which yield:

$$Damage\ Function = 4313.82\,e^{1.22 \cdot ARRI} + 1221.73\,e^{4.94 \cdot IRRI} \tag{3.2}$$

The Damage Function (Equation 3.2) is in terms of ARRI and IRRI. ARRI is the mean amount of in millimeters divided by the mean daily accumulated q_{90} and IRRI is the mean maximum intensity divided by the mean daily accumulated q_{90} as mentioned in Chapter 2.2.2. The performance of the Damage Function is shown in Table 3.3, it has an $R^2 = 0.802$ and Root Square Mean Error ($RSME = 102.5 \times\ 10^6$ USD), with 35 observed flash floods.

Table 3.3: Performance of the Damage Function.

R-squared (R^2)	0.8022
RMSE	102.5×10^6 USD
Number of Observations	35

3.2 Discussion

Given the two previous world studies regarding floods need to consider the different methodologies, periods, and variables. The first thing to consider before comparing our results to Dilley (2005) and Fang et al. (2015), is that both studies are done on general floods, which are not necessarily caused by rainfall as mentioned in Chapter 2.1.1. Nonetheless, they are the only public examples that comprehensively analyze floods from a global perspective and serve as a reference of comparison to the results obtained in this thesis.

Figure 3.12 uses the period 1985 - 2003, and as a parameter for floods, if it was counted as an extreme flood event by Darthmouth Flood Observatory (2023) it was considered a flood by Dilley (2005). Figure 3.12 has a spatial resolution of $1° \times 1°$. Meanwhile, in Figure 3.13, their approach is more complex as they calculated different return periods, particularly the 20yr return period, and their population risk is a measure of a hazard index that implicitly contains the flood times population exposure index with a spatial resolution of $1° \times 1°$.

Regardless of the methodology, period, and source of the flood database, the distribution of flash floods (Figure 3.2) generally coincides with the distribution hotspots for floods in Figure 3.12 and Figure 3.13. All three have India, Southeast Asia, Central Asia, Southeast China, Mozambique, Central America, the Caribbean, Texas in the USA, Southeast Brazil, Northeast Argentina-Uruguay, and Southeast Australia in the upper half tier for risk/occurrence of floods. Particularly, the differences between Figure 3.2 and Figure 3.12 are Mongolia, Iraq, Ukraine, Slovakia, Venezuela, and the Andes countries (except for Ecuador). These discrepancies are most likely because they were not flash floods. They may have been caused by different factors other than rain or belong to other flood subtypes.

Between 2001 and 2020, the countries that experienced more flash floods were Central and Southeast Asia. The five most affected countries by flash floods are Indonesia (29), the Philippines (26), Pakistan (14), Afghanistan (12), and India (12), as shown in Table 3.1 and in Figure 3.3. Comparing this result to Figure 3.13, India, Pakistan, Indonesia, and the Philippines do not appear in the top tier of risk for floods in a 20-year return period, and Afghanistan does not appear at all. Another noticeable absence is the countries in the Mediterranean region, except for Egypt, Syria, and Lebanon, which do not appear in Figure 3.3. These differences are probably due in part to the fact that Fang et al. (2015) weighs proximity to rivers in its risk estimation.

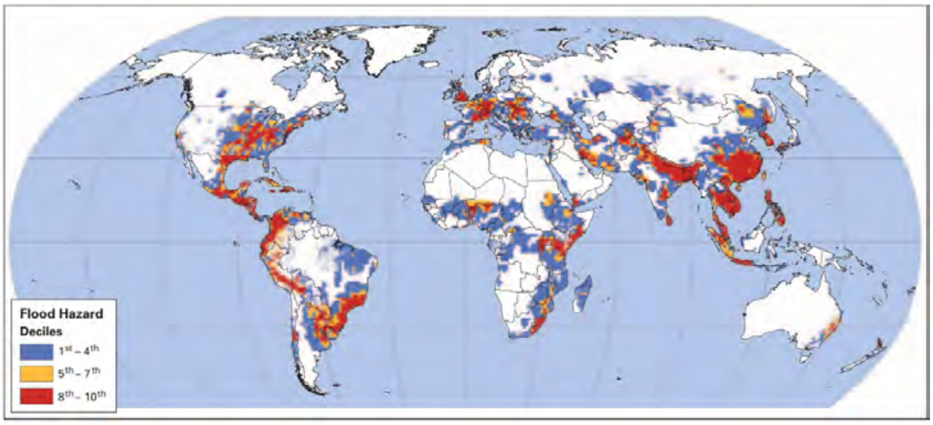

Figure 3.12: Distribution of Flood-prone areas across the World. Source: Dilley (2005)

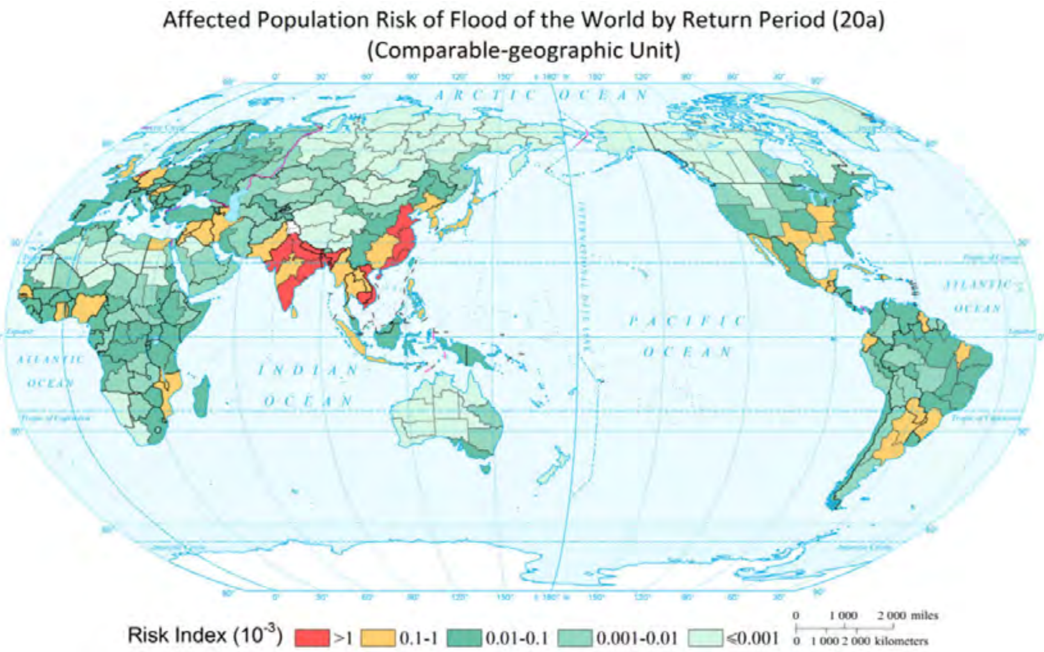

Figure 3.13: Affected Population Risk of Flood of the World by 20-year Return Period. Source: Fang et al. (2015)

3.2.1 The Cost of Flash Floods and The Damage Function

Figure 3.1 illustrates that from a total of **1002**, 834 are left of which 302 with reported damages in USD, which is a survival rate of ≈ 30%. These events are re-analyzed by event and country to generate Figure 3.9. Pakistan emerges as the most heavily affected country, leading the tally with damages exceeding

8 billion USD, trailed by France, China, India, and the United States of America.

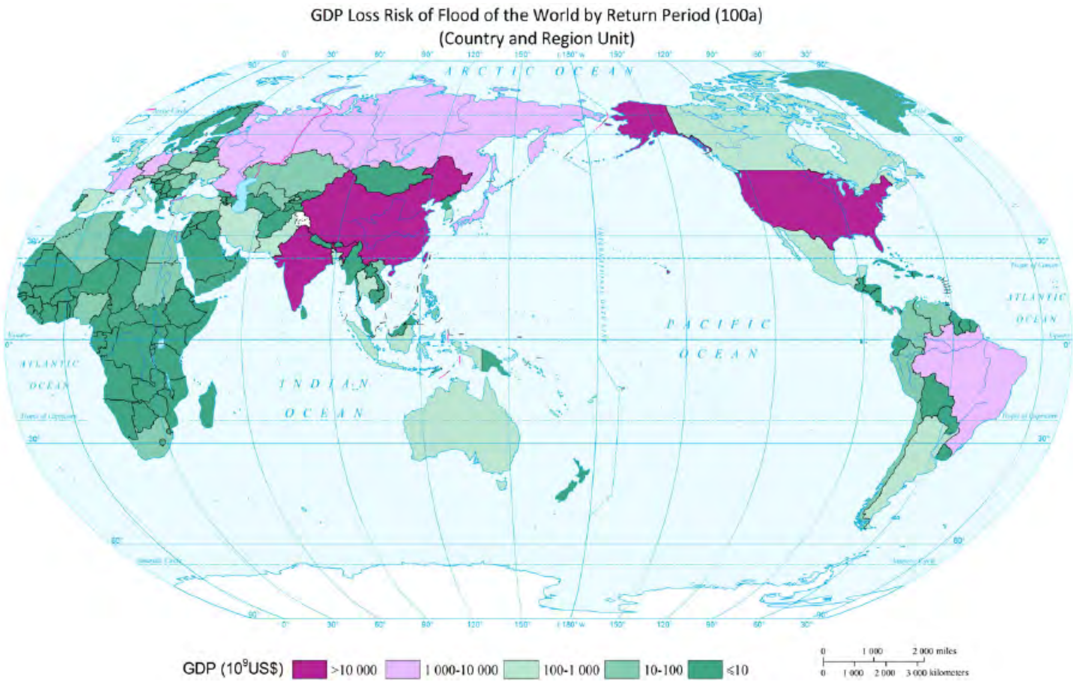

Figure 3.14: Distribution of Flood Risk to GDP Loss in 10^9 USD across the World. Source: Fang et al. (2015)

Irrespective of the specific values, Figure 3.14 represents the anticipated GDP loss over a 100-year return period. This figure bears similarity to Figure 3.9 in that both depict France, China, India, and the United States of America as among the most affected countries. Nonetheless, there are discrepancies as Pakistan, Japan, and Germany differ.

The Damage Function (Equation 3.2) was created by using the most costly flash flood per country. These events range from Somalia with one flash flood damaging in the range of 10^4 USD, with the top five most costly events occurring in Pakistan (over in billion USD, 10^{10} USD), China, India, the United States of America, and France (all with damages in 10^9 USD range).The performance of the Damage Function is shown in Table 3.3; it has an $R^2 = 0.802$ and Root Square Mean Error ($RSME = 102.5 \times\ 10^6$ USD), with 35 observed flash floods. Although it represented the overall behavior of the most costly flash floods per country, it only had 35 observations and substantial RSME. Most probably, adding an economic term that takes into account the country might reduce the error.

3.2.2 Regional Perspective

When considering the duration of flash floods recorded in EM-DAT, it becomes evident that most of these events had a median duration of under one day across all regions. Additionally, across all regions, the mean maximum intensity of these events consistently exceeds 5 mm/hr, aligning with the minimum threshold for flash floods. Interestingly, while most regions exhibit their lowest Accumulative Rainfall Relative Index (ARRI) values at or below 1, the mean ARRI for all regions is approximately 2 or higher.

The regions divided in Table 3.2 show Southeast Asia is the most prone to flash floods, registering an alarming 95 incidents, making it the region with the highest frequency. Followed by the Mediterranean Basin region, Central South Asia, and Georgia, both tied with 45 occurrences. East Africa has experienced 28 flash floods in the fourth position, while Latin America has the fifth spot with 25 recorded incidents. West Africa has 16 flash floods, and East Asia comprises only 11 counts of occurrences.

Southeast Asia has the largest mean values of ARRI, indicating the most accumulative relative rainfall during flash floods. This region experiences, on average, the most intense storms in terms of their rainfall compared to other regions in the dataset. However, it is noteworthy that the Mediterranean region is not far behind regarding mean ARRI values and storm intensity. Both regions exemplify the significant impact of intense rainfall events in triggering flash floods, although their meteorological drivers and frequencies differ significantly.

The maximum value of ARRI occurred in the Mediterranean region, Tunisia, where it rained 17.61 times the q_{90} daily accumulated. Despite this, the region with the largest values of ARRI is Southeast Asia, followed by the Mediterranean. In contrast, the minimum value of ARRI happened in Central South Asia and Georgia in the Islamic Republic of Afghanistan.

The most significant value of the mean maximum intensity during an event occurred in Tunisia with an impressive amount of 65mm in one hour, succeeded by a flash flood in Southeast Asia and another in Central South Asia and Georgia. In contrast, a flash flood in Bolivia had a mean maximum of 1.21 mm/hr, the lowest registered. All region means surpass 5mm/hr; this also holds for the median. However, Southeast Asia and Latin America have means and medians between 10 and 15mm/hr; the rest have one or both values below 10mm/hr.

Flash Floods and Monsoon Regions

Worldwide monsoons are characterized by the seasonal reversal of large-scale surface winds and heavy precipitation associated with the monsoon onset (Krishnamurti et al., 2013). Monsoonal rain patterns extend throughout the tropics, from Northern Oceania, East, Southeast, and Central Asia to parts of Africa, South America, and North America. The dynamic interaction between ocean-atmosphere-land characteristics of an onset monsoon creates the perfect conditions for flash floods. It is no coincidence that a significant number of flash floods from Figure 3.2 fit in the regions analyzed by the Coordinated Downscaled Regional Experiment in Figure 3.15.

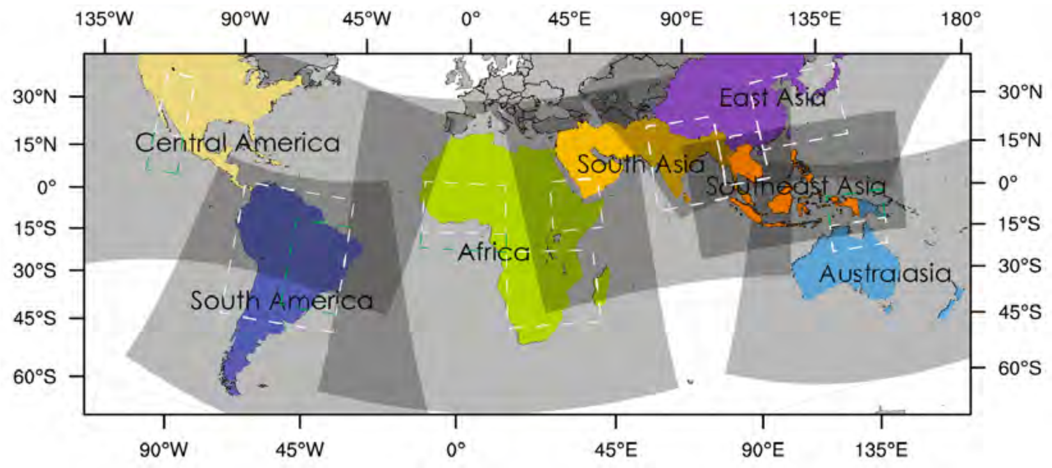

Figure 3.15: Each domain's colored land area represents the regions used for the simulations in the Coordinated Downscaled Regional Experiment (CORDEX) with the Regional Climate Model (RegCM) and the Boxes are the Monsoonal Areas. Source: Ashfaq et al. (2021)

The Mediterrenean

The Mediterranean was after Southeast Asia, the region with the most flash floods, with 45 occurrences, and had a median ARRI higher than Southeast Asia. This suggests that flash floods in the Mediterranean tend to be relatively more severe, underscoring the region's vulnerability to intense precipitation and subsequent flooding. Another factor that could exacerbate is the runoff caused by dry and baked soils, as Thompson (2023) mentions. Given that the Mediterranean coast in the north of Africa, on average, has between 50 to over 175 consecutive dry days, as illustrated in Figure 3.16. Thus, this region is vulnerable due to the mix of severe rainfall, dry soil, and limited infrastructure, particularly in North African countries.

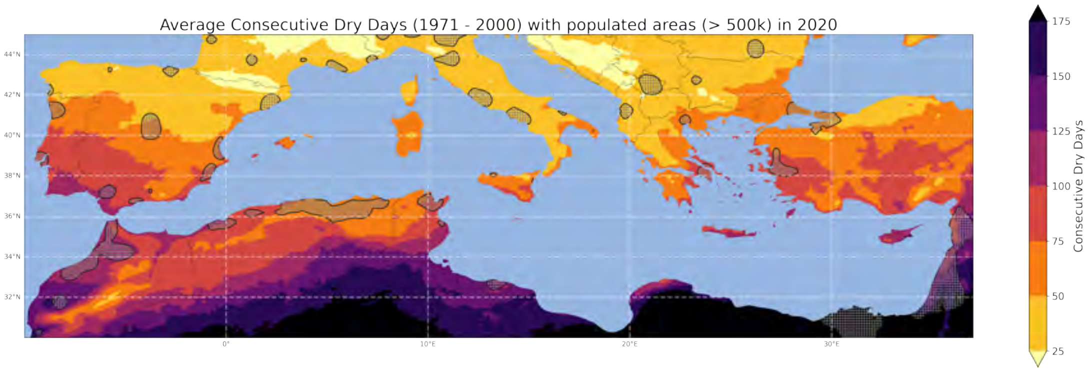

Figure 3.16: Yearly Average Precipitation (1971 - 2000) with hatched areas of Populations over 500,000 in 2020. Map made with the Consecutive Dry Days Index data from ERA-5 from ECMWF.

Latin America and Africa

There is a great deal of uncertainty in the estimations of extreme precipitation in many areas due to the fragile monitoring network (Kundzewicz et al., 2014). Although not exclusive to Latin America and Africa regions, the difference between Figure 3.2 and Figure 3.8 exemplifies that most events did not report damages for these two regions. This underreporting leads to a bias in analyzing flood events and their impacts. These biases have been noticed in the scientific community.

An assessment of research on floods done by Pinos and Quesada-Román (2022) mentions that in the period 2000 - 2020, 302 flood-related English research papers only in Latin America, 16 of those contained the keywords “Flash Floods” directly. World Meteorological Organization (2021) mentions that in South America, extreme rainfall events led to flooding and landslides affecting thousands of people. This is true from a regional to a local perspective; as Viteri López and Morales Rodriguez (2020) points out, in Sao Paulo, flash floods tend to occur in the summer, devastatingly affecting the city’s economy and affecting mainly the citizens of vulnerable neighborhoods.

Also, damages are being underreported not only in EM-DAT but also in the occurrences of flash floods themselves. For example, one significant outcome of the study for Jamaica by Collalti et al. (2023) was identifying an IDF curve, which indicated the likelihood of flash flood events. This threshold corresponded to a return period of 2.17 years. This means we can expect a flash flood in Jamaica every three years; however, there is no flash flood event in Jamaica. In Africa, the effects of catastrophic disasters are likely to go unreported in EM-DAT compared to other continents (CRED, 2022).

Of the ten countries most affected from 2000 to 2019, according to Eckstein et al. (2021), three countries/regions are from Latin America, and one is from Africa. Specifically, Puerto Rico/USA (1), Haiti (3), The Bahamas (6), and Mozambique (5) are among the most affected. This discrepancy can be attributed to two main factors Eckstein et al. (2021) considers other hydrometeorological phenomena than heavy/extreme rainfalls and the fact that most likely flash floods are underreported in EM-DAT for these regions. This affects the overall analysis and must be interpreted with caution.

3.2.3 Limitations to Consider

The results obtained from the analysis of flash flood events from 2001 to 2020, after quality control on the EM-DAT database, reveal several vital insights and shortcomings.

- Global flood data sources,
- Geopy, and the *Nearest Neighbor* method,
- Period of twenty years.

Global databases are getting better with time; nonetheless, they are currently with some limitations. In an assessment done by Jones et al. (2022) for natural hazards between 1990 and 2020, a significant percentage of missing data was present in the EM-DAT. This was especially noticeable when reporting economic losses: 41.5%

The data provided by EM-DAT does not consistently include the A2-level (county or city level), which poses challenges for the georeferencing process and must be discarded. Geopy, while a valuable tool, occasionally encountered difficulties in identifying the city or county for specific countries, further complicating the georeferencing process. Additionally, the utilization of the *Nearest Neighbor* method in IMERG implies a one-dimensional approach that may not fully capture the extent of damage caused by a flash flood event. This limitation is exemplified in the case of the 2010 flood in Pakistan (Figure 3.4), where the red dots represent the georeferenced points from Geopy. Integrating data from IMERG enables the visualization of rainfall amount and distribution.

In contrast, using LITPOP data extracted with CLIMADA provides insights into the distribution of GDP related to nightlights. The overlay of these two datasets suggests that an area-based approach might offer a more comprehensive understanding of the impact of a flash flood event. However, although natural disasters frequently result in significant financial losses, it is unclear how much of these losses will be translated into appreciably lower development rates for individual nations (Strobl, 2012). Even under these circumstances, the situation may not be straightforward.

The twenty-year duration period under consideration falls below the thirty-year climatological normal, which would allow us to discard natural variability. Often, trustworthy time series on the frequency or magnitude of floods are too brief to draw firm conclusions about trends Merz et al. (2010), and with only twenty years, by definition, you cannot get many occurrences of extreme events per country. However, it is a trade-off to work with the latest and best data available.

Chapter 4

Conclusion

In conclusion, this research provides a distinct analysis of flash floods from a global perspective, highlighting the complex nature of flood risk assessment. It is essential to acknowledge its limitations. Challenges related to global flood data sources, georeferencing, underreporting, and the relatively short 20-year analysis period introduce uncertainties in the findings.

Southeast Asia emerges as the most prone region, with 95 recorded incidents, followed by the Mediterranean Basin, Central South Asia, and Georgia, each with 45 occurrences (Table 3.2). These findings emphasize the need for tailored strategies to mitigate the impact of flash floods in these high-risk regions.

The regional perspective sheds light on flash floods' unique differences and similarities worldwide. For example, Southeast Asia is characterized by intense rainfall and high ARRI values. A further analysis of global flash floods also underscores a relationship between monsoon regions and flood occurrence. The dynamic interaction between ocean-atmosphere-land during monsoon onset creates suitable conditions for intense rainfall and subsequent flash flooding. This type of rainfall pattern extends across various tropical regions, including Northern Oceania, East and Southeast Asia, Central Asia, parts of Africa, South America, and North America. This is evident in the spatial distribution of flash floods, which greatly aligns with the regions affected by monsoons. Understanding the relationship between monsoons and flash floods is crucial for anticipating and mitigating the impact of these events in vulnerable regions.

The Mediterranean region also exhibits high vulnerability due to relatively severe rainfall. Latin America and Africa face challenges related to underreporting of flash floods and associated damages, highlighting the need for improved data collection and reporting.

The economic costs associated with flash floods confirm that they have significant financial implications, with countries like Pakistan, France, China, India, and the USA experiencing substantial damages. While the damage function demonstrates a relatively high degree of explanatory power ($R^2 = 0.802$), it also indicates a substantial root mean square error ($RMSE = 102.5 \times 10^6$ USD), suggesting some limitations in accurately predicting the economic impact of flash floods.

Chapter 5

A Future Perspective on Flash Floods

Research has shown that human-induced climate change has exacerbated extreme precipitation events. If global warming persists, the atmosphere's capacity to hold water vapor will continue to expand, increasing by 7 % per each 1 °C of warming (IPCC, 2022b). This is expected to accelerate the water cycle, making extreme precipitation events more regular and disproportionately increasing the probabilities of impacts and losses to natural and human systems (IPCC, 2022c). Thus adapting to climate change is required. These adaptions may come in the form of implementing early warning systems, improving infrastructure, establishing a legal framework, and financial instruments to rapidly allocate capital to rehabilitate damaged assets. As of today, 1-day heavy precipitation events are 1.3 times more likely to occur than in the preindustrial average over land and the likelihood of flash floods increases with every increment in temperature (IPCC, 2022b) and this upward trend can be seen in Figure 5.1.

Alfieri et al. (2017) found that increased global air temperatures will intensify the hydrological cycle, leading to more intense rainfall worldwide. Kundzewicz et al. (2014) projects that from 2071 to 2100, the majority of southern South America and western Amazonia will experience more intense episodes of extreme precipitation. Under the most optimistic scenario (RCP2.6-SSP1) of the Paris Agreement targets, Kam et al. (2021) found that riverine floods are anticipated to double (+110%) by the end of this century, increasing the average risk of population displacement. Additionally, Merz et al. (2010) states that if the current climate and future weather patterns are similar, hourly extreme precipitation occurrences are expected to rise dramatically in practically all geographical regions of North America.

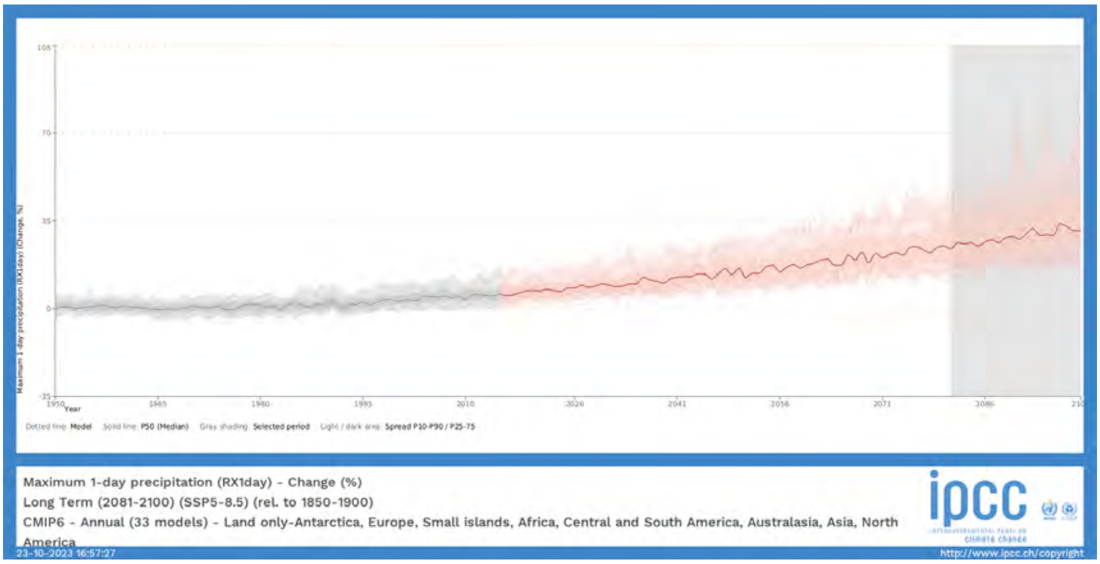

Figure 5.1: The maximum one-day precipitation (RX1day) time series for the period 2081-2100 under the SSP-8.5 scenario, focusing specifically on land-based data. Source: IPCC (2022b)

Bibliography

Alfieri, L., Bisselink, B., Dottori, F., Naumann, G., De Roo, A., Salamon, P., Wyser, K., and Feyen, L. (2017). Global projections of river flood risk in a warmer world, earth's future, 5, 171–182.

Ashfaq, M., Cavazos, T., Reboita, M. S., Torres-Alavez, J. A., Im, E.-S., Olusegun, C. F., Alves, L., Key, K., Adeniyi, M. O., Tall, M., et al. (2021). Robust late twenty-first century shift in the regional monsoons in regcm-cordex simulations. *Climate Dynamics*, 57:1463–1488.

Beck, H. E., Zimmermann, N. E., McVicar, T. R., Vergopolan, N., Berg, A., and Wood, E. F. (2018). Present and future köppen-geiger climate classification maps at 1-km resolution. *Scientific data*, 5(1):1–12.

Bernet, D. B., Prasuhn, V., and Weingartner, R. (2017). Surface water floods in switzerland: what insurance claim records tell us about the damage in space and time. *Natural Hazards and Earth System Sciences*, 17(9):1659–1682.

Bernet, D. B., Trefalt, S., Martius, O., Weingartner, R., Mosimann, M., Röthlisberger, V., and Zischg, A. P. (Celebrating 50 Years of Disaster Epidemiological Research, Data Collection, and International Cooperation2019). Characterizing precipitation events leading to surface water flood damage over large regions of complex terrain. *Environmental Research Letters*, 14(6):064010.

Brakenridge, R. (2023). Darthmouth flood observatory: Mission.

CCRIF (2016). The ccrif excess rainfall (xsr 2.5) model.

Ciullo, A., Strobl, E., Meiler, S., Martius, O., and Bresch, D. N. (2023). Increasing countries' financial resilience through global catastrophe risk pooling. *Nature Communications*, 14(1):1–9.

CLIMADA (2023). Climada overview. Accessed: September 14, 2023.

Collalti, D., Spencer, N., and Strobl, E. (2023). Flash flood detection via copula-based idf curves: Evidence from jamaica. *Natural Hazards and Earth System Sciences Discussions*, 2023:1–22.

CRED (2022). The interplay of drought-flood extreme events in africa over the last twenty years (2002-2021). *CRED Crunch*.

CRED and IRSS (2023). Celebrating 50 years of disaster epidemiological research, data collection, and international cooperation. *CRED*.

Darthmouth Flood Observatory (2023). Space-based measurement, mapping, and modeling of surface water: For research, humanitarian, and water resources applications.

De Janvry, A., Del Valle, A., and Sadoulet, E. (2016). Insuring growth: the impact of disaster funds on economic reconstruction in mexico. *World Bank Policy Research Working Paper*, (7714).

Dilley, M. (2005). *Natural disaster hotspots: a global risk analysis*, volume 5. World Bank Publications.

Eckstein, D., Künzel, V., and Schäfer, L. (2021). *The Global Climate Risk Index 2021.* Bonn: Germanwatch.

EM-DAT (2023). Em-dat documentation: Classification glossary. Accessed on October 18, 2023.

Environment Canada (2020). Criteria for public weather alerts. Accessed: April 17, 2023.

European Flood Awareness System (2023). European flood awareness system. Accessed on December 30, 2023.

Fang, J., Li, M., and Shi, P. (2015). *Mapping Flood Risk of the World*, pages 69–102. Springer Berlin Heidelberg, Berlin, Heidelberg.

Gautam, A. K. and Pandey, A. (2022). Ground validation of gpm day-1 imerg and tmpa version-7 products over different rainfall regimes in india. *Theoretical and Applied Climatology*, 149(3-4):931–943.

GeoPy Contributors (2018). Welcome to geopy's documentation! Accessed on September 26, 2023.

India Meteorological Department (2022). Frequently asked questions. Accessed on October 18, 2023.

INSURESILIENCE, P.-P. F. O. (2016). Climate risk insurance for the poor & vulnerable.

IPCC (2022a). *Climate Change 2022: Impacts, Adaptation and Vulnerability. Contribution of Working Group II to the Sixth Assessment Report of the Intergovernmental Panel on Climate Change.* Cambridge University Press, Cambridge, UK and New York, NY, USA.

IPCC (2022b). *Summary for Policymakers. In: Climate Change 2022: Mitigation of Climate Change. Contribution of Working Group I to the Sixth Assessment Report of the Intergovernmental Panel on Climate Change.* Cambridge University Press, Cambridge, UK and New York, NY, USA.

IPCC (2022c). *Summary for Policymakers. In: Climate Change 2022: Mitigation of Climate Change. Contribution of Working Group III to the Sixth Assessment Report of the Intergovernmental Panel on Climate Change*. Cambridge University Press, Cambridge, UK and New York, NY, USA.

Jones, R. L., Guha-Sapir, D., and Tubeuf, S. (2022). Human and economic impacts of natural disasters: can we trust the global data? *Scientific data*, 9(1):572.

Jonkman, S. N. (2005). Global perspectives on loss of human life caused by floods. *Natural hazards*, 34(2):151–175.

Justiniano, I., Boyer, M., Gunasekera, R., and Humbert, T. (2021). Disaster risk financing in the caribbean region-framework and assessments.

Kam, P. M., Aznar-Siguan, G., Schewe, J., Milano, L., Ginnetti, J., Willner, S., McCaughey, J. W., and Bresch, D. N. (2021). Global warming and population change both heighten future risk of human displacement due to river floods. *Environmental Research Letters*, 16(4):044026.

Koks, E. E. and Thissen, M. (2016). A multiregional impact assessment model for disaster analysis. *Economic Systems Research*, 28(4):429–449.

Krishnamurti, T. N., Stefanova, L., and Misra, V. (2013). *Monsoons*, pages 75–119. Springer New York, New York, NY.

Kundzewicz, Z. W., Kanae, S., Seneviratne, S. I., Handmer, J., Nicholls, N., Peduzzi, P., Mechler, R., Bouwer, L. M., Arnell, N., Mach, K., Muir-Wood, R., Brakenridge, G. R., Kron, W., Benito, G., Honda, Y., Takahashi, K., and Sherstyukov, B. (2014). Flood risk and climate change: global and regional perspectives. *Hydrological Sciences Journal*, 59(1):1–28.

le Polain de Waroux, O. (2011). Floods as human health risks. In Nriagu, J., editor, *Encyclopedia of Environmental Health*, pages 744–755. Elsevier, Burlington.

Liang, Y., Wang, Y., Zhao, Y., Lu, Y., and Liu, X. (2019). Analysis and projection of flood hazards over china. *Water*, 11(5):1022.

Merz, B., Hall, J., Disse, M., and Schumann, A. (2010). Fluvial flood risk management in a changing world. *Natural Hazards and Earth System Sciences*, 10(3):509–527.

Mexican National Weather Service (2023). Mexican national weather service webpage. Accessed on November 20, 2023.

Microsoft Open Source, McFarland, M., Emanuele, R., Morris, D., and Augspurger, T. (2022). microsoft/planetarycomputer: October 2022.

NASA (2023). The tropical rainfall measuring mission (trmm). Accessed: September 14, 2023.

National Weather Service (2022). Flash floods and floods...the awesome power! Accessed on November 20, 2023.

OpenStreetMap Foundation (2023). Openstreetmap. Accessed on September 26, 2023.

Panda, A. and Surminski, S. (2020). *Climate and Disaster Risk Insurance in Low Income Countries: Reflections on the Importance of Indicators and Frameworks for Monitoring the Performance and Impact of CDRI*. Grantham Research Institute on Climate Change and the Environment.

Pinos, J. and Quesada-Román, A. (2022). Flood risk-related research trends in latin america and the caribbean. *Water*, 14(1).

Science Insider (2023). In colorado, a global flood observatory keeps a close watch on harvey's torrents.

Strobl, E. (2012). The economic growth impact of natural disasters in developing countries: Evidence from hurricane strikes in the central american and caribbean regions. *Journal of Development Economics*, 97(1):130–141.

Stull, R. B. (1988). *An introduction to boundary layer meteorology*, volume 13. Springer Science & Business Media.

Tellman, B., Sullivan, J. A., Kuhn, C., Kettner, A. J., Doyle, C. S., Brakenridge, G. R., Erickson, T. A., and Slayback, D. A. (2021). Satellite imaging reveals increased proportion of population exposed to floods. *Nature*, 596(7870):80–86.

The Floodlist Team (2023). The floodlist team. Accessed on December 30, 2023.

The Global Flood Database (2022). The global flood database. Accessed on December 30, 2023.

Thompson, R. (2023). Drought: heavy rain now might be a serious problem for the uk's parched landscape. Accessed on December 20, 2023.

UCAR/COMET (2011). Introduction to tropical meteorology. Accessed on October 20, 2023.

UNICEF (2023). Flooding in kalehe territory, south kivu province, drc. *Flash Flood Report*, 6.

United Nations (2015). Sendai framework for disaster risk reduction 2015-2030. Accessed: April 6, 2023.

United Nations (2019). Un climate action summit: Resilience and adaptation strand insuresilience global partnership. Accessed: April 6, 2023.

United Nations Framework Convention on Climate Change (2015). The paris agreement. Accessed on April 6, 2023.

United Nations Office for Disaster Risk Reduction (2020). *Human Cost of Disasters: An Overview of the Last 20 Years 2000-2019*. UN Office for Disaster Risk Reduction.

United Nations Office for Disaster Risk Reduction (2022). *Global assessment report on disaster risk reduction 2022: Our world at risk: Transforming governance for a resilient future*. UN.

Viteri López, A. S. and Morales Rodriguez, C. A. (2020). Flash flood forecasting in são paulo using a binary logistic regression model. *Atmosphere*, 11(5):473.

World Meteorological Organization (2021). Estado del clima en américa latina y el caribe 2021.

WPC (2023). Excessive rainfall outlooks (eros). Accessed: September 17, 2023.

Appendix A

Regional Perspective to Extreme and/or Excessive Rainfall

A.1 World 1-day Accumulated Quantiles

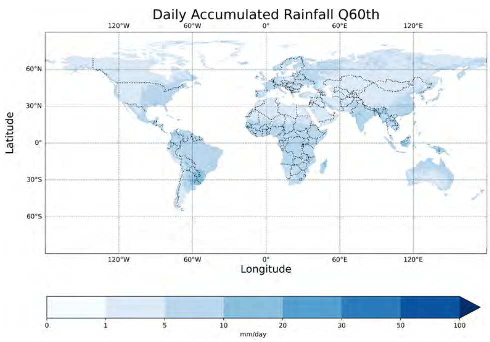

Figure A.1: 60^{th} Quantile.

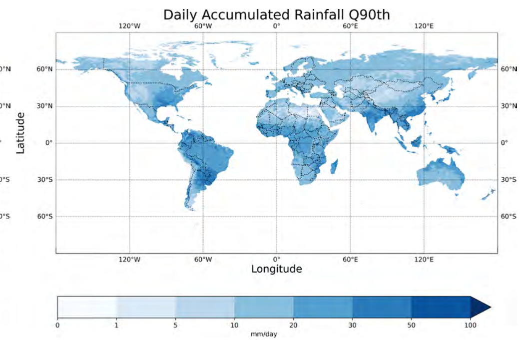

Figure A.2: 90^{th} Quantile.

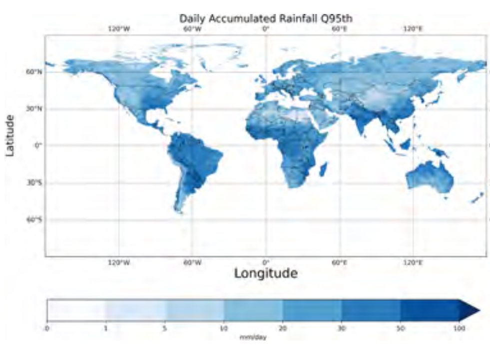

Figure A.3: 95^{th} Quantile.

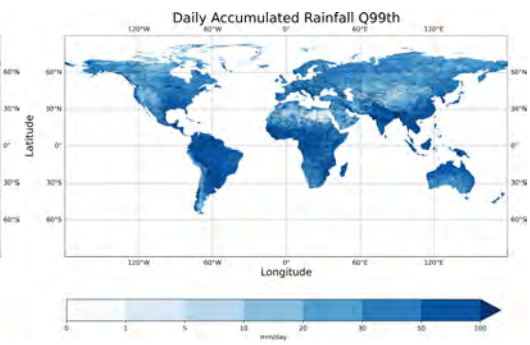

Figure A.4: 99^{th} Quantile.

1-Day Accumulated Rainfall Quantiles in millimeters for the 2001 - 2020 Period.

Contained within this appendix is a curated repository of rainfall thresholds originating from diverse geographical locales. While it does not constitute an exhaustive compilation, it is a comprehensive reference encompassing distinct criteria employed worldwide to delineate the distinction between ordinary precipitation and the extraordinary. Originating from regions as varied as the lofty Himalayas to the arid Sahelian landscapes, these thresholds amalgamate the collective wisdom of time-honored traditions and contemporary scientific methodologies. It is imperative to acknowledge that this compendium serves as a guiding reference.

A.2 Brazil

Table A.1: Rainfall Thresholds in Brazil.

Region or Area Name	**Duration (hrs)**	**Intensity (mm/hr)**	**Accumulated (mm)**
Sao Paolo Metropolitan Area[1]	-	30	30 mm

Sources:

1. Viteri López and Morales Rodriguez (2020)

A.3 The Caribbean Catastrophe Risk Insurance Facility (CCRIF)

Table A.2: Rainfall Thresholds in CCRIF.

Region or Area Name	**Duration (hrs)**	**Intensity (mm/hr)**	**Accumulated (mm)**
Caribbean[1]	12 – 48	-	40
Central America[1]	24 – 72	-	40

Sources:

1. CCRIF (2016)

A.4 Canada

A.4.1 Summer

Table A.3: Summer Short Rainfall Thresholds for Canada.

Region or Area Name	**Duration (hr)**	**Intensity(mm/hr)**	**Accum(mm)**
Alberta, Saskatchewan, Manitoba, Ontario, and Quebec (except Nunavik)	1 *	50	-
Interior dry sections of British Columbia		15	
Remaining sections of British Columbia, Yukon, Northwest Territories, Nunavut, New Brunswick, Prince Edward Island, Nova Scotia, Newfoundland and Labrador		25	

Table A.4: Summer Long Rainfall Thresholds for Canada.

Region or Area Name	**Duration (hr)**	**Intensity(mm/hr)**	**Accum (mm)**
National, except Nunavik* and portions of British Columbia	24	-	50
Interior dry sections of British Columbia			15
Inland Vancouver Island, West Vancouver Island, North Vancouver Island, Central Coast - coastal sections, and North Coast - coastal sections			100
National (except Nunavik) and portions of British Columbia	48	-	75

A.4.2 Winter

Comments:

- The thresholds are divided by region and by intensity or duration.

Sources:

1. Environment Canada (2020).

Table A.5: Summer Short Rainfall Thresholds for Canada.

<table>
<tr><th>Region or Area Name</th><th>Duration (hr)</th><th>Intensity(mm/hr)</th><th>Accum(mm)</th></tr>
<tr><td>Alberta, Saskatchewan, Manitoba, Ontario, and Quebec (except Nunavik)</td><td rowspan="3">1 *</td><td>50</td><td rowspan="3">-</td></tr>
<tr><td>Interior dry sections of British Columbia</td><td>15</td></tr>
<tr><td>Remaining sections of British Columbia, Yukon, Northwest Territories, Nunavut, New Brunswick, Prince Edward Island, Nova Scotia, Newfoundland and Labrador</td><td>25</td></tr>
</table>

Table A.6: Summer Long Rainfall Thresholds for Canada.

<table>
<tr><th>Region or Area Name</th><th>Duration (hr)</th><th>Intensity(mm/hr)</th><th>Accum (mm)</th></tr>
<tr><td>National, except Nunavik* and portions of British Columbia</td><td rowspan="3">24</td><td rowspan="3">-</td><td>50</td></tr>
<tr><td>Interior dry sections of British Columbia</td><td>15</td></tr>
<tr><td>Inland Vancouver Island, West Vancouver Island, North Vancouver Island, Central Coast - coastal sections, and North Coast - coastal sections</td><td>100</td></tr>
<tr><td>National (except Nunavik) and portions of British Columbia</td><td>48</td><td>-</td><td>75</td></tr>
</table>

A.5 China

Table A.7: Rainfall Thresholds for China.

Region or Area Name	Duration (hrs)	Intensity (mm/hr)	Accumulated (mm)
China	24	- -	$\geqslant q_{60}$ * $\geqslant q_{95}$ **

Comments:

- *Criteria for flood.
- **Criteria for serious flood

Sources:

1. Liang et al. (2019).

A.6 India

Table A.8: Rainfall Thresholds in India.

Region or Area Name	Duration (hrs)	Intensity (mm/hr)	Accumulated (mm)
India[1]	24	-	$\geqslant q_{60}$

Comments:

- Excess rainfall, is 60% relative to the long period average of each spot.

Sources:

1. India Meteorological Department (2022)

A.7 Mexico

Table A.9: Rainfall Thresholds For Mexico.

Region or Area Name	Duration (hrs)	Intensity (mm/hr)	Accumulated (mm)
Mexico[1]	24	-	$\geqslant q_{90}$
Mexico[2]	24	-	25

Sources:

1. De Janvry et al. (2016)
2. Mexican National Weather Service (2023)

Table A.10: Rainfall Thresholds in Switzerland.

Region or Area Name	**Duration (hrs)**	**Intensity (mm/hr)**	**Accumulated (mm)**
Switzerland[1]	-	$\geqslant q_{90}$	$\geqslant q_{98}$

A.8 Switzerland

Comments:

- Emphasizes the use of the quantiles for each point of interest.

Sources:

1. Bernet et al. (2019)

A.9 United States of America

Table A.11: Rainfall Thresholds for the United States of America.

Region or Area Name	**Duration (hrs)**	**Intensity (mm/hr)**	**Accumulated (mm)**
U.S.A.[1]	-	-	-

Comments:

- Estimation of specific rainfall amounts would fill each river and stream to the bank.

Sources:

1. WPC (2023)

A.10 World

Table A.12: Rainfall Thresholds for the entire World.

Region or Area Name	**Duration (hrs)**	**Intensity (mm/hr)**	**Accumulated (mm)**
World[1]	72	-	$\geqslant q_{95}$

Comments:

- Criteria for extreme precipitation.

Sources:

1. Fang et al. (2015)